Contract No. Nonr 839(38)

NONEQUILIBRIUM STRUCTURE OF HYDROMAGNETIC GAS-IONIZING SHOCK FRONTS IN ARGON

by

Martin I. Hoffert

FEBRUARY 1967

POLYTECHNIC INSTITUTE OF BROOKLYN

DEPARTMENT
of
AEROSPACE ENGINEERING
and
APPLIED MECHANICS

PIBAL REPORT NO. 1008

NONEQUILIBRIUM STRUCTURE OF HYDROMAGNETIC GAS-IONIZING SHOCK FRONTS IN ARGON

by

Martin L. Hoffert

The research has been conducted under Contract Nonr 839(38) for PROJECT DEFENDER, and was made possible by the support of the Advanced Research Projects Agency under Order No. 529 through the Office of Naval Research.

Polytechnic Institute of Brooklyn

Department

of

Aerospace Engineering and Applied Mechanics

February 1967

PIBAL Report No. 1008

BLANK PAGE

NONEQUILIBRIUM STRUCTURE OF HYDROMAGNETIC GAS-IONIZING SHOCK FRONTS IN ARGON[†]

by

Martin I. Hoffert[‡]

Polytechnic Institute of Brooklyn

SUMMARY

This study deals analytically with the structure of gas-ionizing hydromagnetic shock waves. Since these waves, by definition, must have non-electrically-conducting upstream states, their existence at very high shock temperatures must be ruled out on the physical grounds that forward-radiated precursor ionization makes the unshocked gas conducting. A "low temperature" collisionally-ionizing shock with oblique magnetic field is studied here to determine whether certain concepts which exist in the current literature are relevant. Nondimensionalized equations governing the nonequilibrium structure of such a front propagating into un-ionized argon are formulated using ionization rates and an electron energy equation developed in an earlier paper. Comparison of the magnitudes of viscous and magnetic Reynolds numbers within this front indicates that, if a structure exists, it must consist of a narrow "imbedded" viscous shock standing upstream of a much wider hydromagnetic interaction and ionization relaxation zone. Hence, a modified form of the Zeldovich-von Neumann-Döring (ZND) approximation is applicable to the structure problem. It is shown that in this approximation nontrivial steady-state structures cannot be constructed for "fast" gas-ionizing shocks. On the other hand, solutions are possible for "slow" waves, and

---

[†]The research has been conducted under Contract Nonr 839(38) for PROJECT DEFENDER, and was made possible by the support of the Advanced Research Projects Agency under Order No. 529 through the Office of Naval Research.

[‡]Graduate Student; also, Senior Scientist, General Applied Science Laboratories, Inc., Westbury, New York.

these are obtained numerically for a family of hydromagnetically oblique shocks at Mach number $M_1 = 20$ and Alfvén number $M_{A_1} = 1/\sqrt{Z}$ with parametrically varied values of the upstream electric field. In contrast to previous expectations, the upstream electric field is not uniquely defined by the structure. Because the slow solutions are effectively exothermic, to the point where their post-shock temperatures are associated with radiation-induced precursor ionization, it seems likely that only the solution with the upstream electric field corresponding to a pure hydromagnetic shock has physical significance.

Table of Contents

Table of Figures

Table of Figures (Contd.)

BLANK PAGE

1. INTRODUCTION

In recent years, a number of investigators have contributed to the formulation of a theoretical model descriptive of the so-called gas-ionizing hydromagnetic shock wave (Kulikovskii and Lyubimov[1-5], Kunkel and Gross[6], Helliwell[7], Chu[8], Woods[9], May and Tendys[10] and Taussig[11, 12]). These waves are thought to exist, for example, in electromagnetic shock tubes. All the aforementioned authors either postulate or imply that the structure of these waves conforms to the following archetype (this description can also be taken as a definition of a "gas-ionizing hydromagnetic shock" in the present context): Upstream, the gas is un-ionized, electrically non-conducting and hence uncoupled from the magnetic fields through which the shock moves. Consequently, the leading edge of the front develops precisely as an ordinary hydrodynamic shock. Because of collisional ionizing reactions associated with the rising temperature, an electrically conducting (hence hydromagnetically active) plasma is created somewhere in the shock interior. It follows that the overall structure is hybrid in nature, being partly hydrodynamic and partly hydromagnetic.

The most distinctive implication of this archetype is that the Rankine-Hugoniot conditions are no longer sufficient to predict the downstream state of the shock in terms of the upstream state and the shock velocity. This is because, in contrast to purely hydromagnetic shocks, the upstream gas-frame electric field is not uniquely defined in terms of the upstream velocity and magnetic fields: As a non-electrical conductor, the unshocked gas is incapable of sustaining a current flow, so the upstream boundary condition of no currents in the undisturbed gas is automatically satisfied for any electric field.

It has been argued that an analytic prediction of the electric field requires an analytic and physically correct solution for the ionizing wave structure[13]. In order to gain some insight into the structure problem, prior studies[1, 8, 10, 13] have assumed temperature-dependent, step-function models for the variation of electrical

conductivity σ within the shock, i.e., $\sigma=0$ for $T'<T^{*\prime}$ and $\sigma\neq 0$ for $T'>T^{*\prime}$, where T' is the gas temperature and $T^{*\prime}$ is some "reference" temperature. Analysis by May and Tendys[10] indicates that shock structure integral curves deduced from this model are applicable only when $T^{*\prime}$ is of the same order-of-magnitude as the characteristic (first) ionization temperature of the unshocked gas.

The present study is concerned with obtaining shock-structure solutions (if any exist) which are consistent with the gas-ionizing archetype and which also incorporate realistic representations of transport and rate processes in a collisionally-ionizing monatomic gas, argon in particular. It is motivated by a realization that by misrepresenting the physics of high temperature gases, the step-function temperature-dependent conductivity approach can give qualitatively misleading results for two different reasons: (1) If the internal shock temperature approaches the ionization temperature, as May and Tendys suggest, the gas becomes fully ionized almost immediately (since each interparticle collision has enough energy on-the-average to "knock off" an outer electron), but at these temperatures radiation-induced precursor ionization levels are sufficiently high so as to preclude any reasonable interpretation of the upstream state as un-ionized[14]. Consequently, the "gas-ionizing" archetype with its implied electric field indeterminacy is violated and the shock is not gas-ionizing, in the present context. (2) Another possibility, the one actually explored in this paper, is that of a "low temperature" gas-ionizing shock, i.e., a front creating a nonequilibrium plasma in which photo-ionization is realistically negligible compared to collisional ionization. In this latter case the conceots embodied in the archetype may still be revelant but the step-function temperature-dependent conductivity model is unrealistic. In fact, the local electrical conductivity depends on the degree of ionization α, as well as temperature, so that ionization-lags in real nonequilibrium flows can have considerable influence on the variation of σ within the shock transition.

The macroscopic global conservation and Maxwell equations used in the

present analysis are developed in Sec. 2. For an electrically conducting upstream state, these can be integrated between upstream and downstream states, to give the usual hydromagnetic jump conditions[15-17]. In order to express the dissipation fluxes (i.e., the stress tensor, heat flux vector and current density vector) in terms of lower-order dependent variables, it is assumed first that the electron cyclotron frequency was always much less than the electron collision frequency. Secondly, the Navier-Stokes approximation is used, together with a two-temperature modification of the Chapman-Enskog expressions for transport coefficients. The first assumption, which rules out Hall currents, is removable in general by using a more general version of Ohm's law[18], but it is justified specifically for the flow conditions of the calculations to be presented later. It is well-known that the Navier-Stokes approximation is questionable in connection with strong hydrodynamic shock structure calculations. Nevertheless, its use in the present study is plausible on the grounds that qualitative misrepresentation of the structure, of the sort introduced by the aforementioned electrical conductivity models, are unlikely; moreover, Navier-Stokes equations have been used, with some success, to study the structure of purely hydromagnetic shocks (Marshall[19], Burgers[20], Ludford[21], Germain[22,23], Bleviss[24], and Anderson[25]).

In Sec. 3, the ionization rates and transport properties of partially ionized nonequilibrium argon are developed in terms of fundamental collision cross-sections. The sole source of electrons is taken to be collisional ionization by the reactions:

$$Ar + Ar \underset{k_{rA}}{\overset{k_{fA}}{\rightleftharpoons}} Ar^+ + e^- + Ar, \tag{1a}$$

$$e^- + Ar \underset{k_{rA}}{\overset{k_{fe}}{\rightleftharpoons}} Ar^+ + e^- + e^-, \tag{1b}$$

where k_{fA}, k_{fe} are the forward ionization rate coefficients and k_{rA}, k_{re} are the

reverse three-body recombination rate coefficients. The kinetics of Eqs. (1a, b) were treated previously in connection with flow in the relaxation zone of a hydrodynamic shock[26]. It is assumed that the plasma remains quasi-neutral throughout so that electrogasdynamic influences on shock structure[27-30] are negligible compared to magnetogasdynamic effects. Because the reaction rates, transport properties and thermodynamics of partially ionized argon depend on both electron and heavy-particle temperatures, an appropriate electron energy equation is required.

Sec. 4 deals with the nature of the shock structure integral curves which are consistent with the gas-ionizing archetype. In this portion, it is suggested that the "ZND" approximation of detonation wave theory is applicable to the present problem and the consequences of this representation are examined for both "fast" and "slow" gas-ionizing shocks. In Sec. 5, selected numerical shock structure solutions are presented and numerical techniques are treated briefly. The conclusions of this investigation are given in Sec. 6, where the applicability and relevance of the present results are discussed and potentially profitable directions of future research are suggested.

2. GLOBAL HYDROMAGNETIC EQUATIONS IN OBLIQUE MAGNETIC FIELD SHOCK GEOMETRIES

We shall be concerned here with the distribution of flow variables within the transition region of the oblique gas-ionizing shock whose geometry, in shock-frame coordinates, is shown in Fig. 1. This shock may be envisaged as having begun its career as an ordinary hydrodynamic gas-ionizing shock which later "penetrated" a region of nonzero magnetic field and subsequently attained a steady-state structure. An (x', y', z') coordinate system is selected in which the upstream magnetic field vector resolves along the x' and z' axes. For the scalar electrical conductivity assumed previously, the shock-frame electric field is in the y' direction and all electromagnetic components which are initially zero, remain zero (the "switch-on" shock is an exception not explicitly considered here).

As a general rule "primes" are used to distinguish physical variables, all of which are in mks units, from the more convenient nondimensionalized variables used later in developing the equations; furthermore, cartesian tensor notation is used to express the general form of the governing equations more concisely. The component directions in the tensor notation are related to the coordinate system of Fig. 1 as follows: $x_1' = x'$, $x_2' = y'$, $x_3' = z'$; $(\ )_1 = (\ )_x$, $(\ )_2 = (\ )_y$, $(\ )_3 = (\ )_z$. In the present rotation δ_{ij} is the usual Kroenecker delta: $\delta_{ij}=1$, if $i=j$; $\delta_{ij}=0$, if $i \neq j$. The symbol ϵ_{ijk} is the permutation tensor: $\epsilon_{ijk}=0$, if $i=j$, $i=k$ or $j=k$; $\epsilon_{ijk}=1$, if ijk are in cyclic order (123, 321, 312) and $\epsilon_{ijk}=-1$, if ijk are unequal but not in cyclic order (132, 213, 321).

The thermodynamic pressure p' and specific enthalpy i' of partially ionized two temperature argon satisfy the equations of state[26]

$$p' = \rho' R (T' + \alpha T_e') , \tag{2}$$

$$i' = \frac{5}{2} R (T' + \alpha T_e') + \alpha R \Theta_{ion}' , \tag{3}$$

where ρ' is the mass density, T' is the heavy particle temperature, T_e'

is the electron temperature, α is the degree of ionization, $R = 2.082 \times 10^2$ joule/kg -.^{o}K is the gas constant for atomic argon and $\Theta'_{ion} = 183,100\ ^{o}K$ is a characteristic temperature for the single ionization of argon.

Using Eqs. (2) and (3) to immediately eliminate pressure and enthalpy, the global conservation and Maxwell equations for the steady flow of a quasi-neutral plasma can be written in divergence form as follows:[25]

$$\frac{\partial}{\partial x'_i} (\rho' u'_i) = 0 \tag{4}$$

$$\frac{\partial}{\partial x'_i} \left[\rho' u'_i u'_j + \rho' R (T' + \alpha T'_e) \delta_{ij} + \frac{1}{\mu_o} \left(\delta_{ij} \frac{B'^2}{2} - B'_i B'_j \right) + \tau'_{ij} \right] = 0, \tag{5}$$

$$\frac{\partial}{\partial x'_i} \left[\rho' u'_i \cdot \frac{5}{2} \cdot R (T' + \alpha T'_e + \frac{2}{5} \cdot \alpha \Theta'_{ion}) + \rho' u'_i \cdot \frac{u'^2}{2} \right.$$

$$\left. + \epsilon_{ijk} \cdot \frac{E'_j B'_k}{\mu_o} + u'_j \tau'_{ij} + q'_i + q'_{e,i} \right] = 0, \tag{6}$$

$$\epsilon_{ijk} \cdot \frac{\partial B'_k}{\partial x'_j} = \mu_o J'_i , \tag{7}$$

$$\epsilon_{ijk} \cdot \frac{\partial E'_k}{\partial x'_j} = 0 , \tag{8}$$

$$\frac{\partial E'_i}{\partial x'_i} = 0 , \tag{9}$$

$$\frac{\partial B_i'}{\partial x_i'} = 0 \quad , \tag{10}$$

where u_i' is the flow velocity, B_i' is the magnetic induction, E_i' is the electric field intensity, $\mu_o = 4\pi \times 10^{-7}$ henry/m is the free space magnetic permeability in mks units, J_i' is the current flux density vector, q_i' and $q_{e,i}'$ are the heavy-particle and electron-gas heat flux vectors and τ_{ij}' is the viscous stress tensor.

As indicated in Sec. 1, a scalar electrical conductivity σ is assumed in this analysis, in which case the relevant form of Ohm's law is

$$J_i' = \sigma(E_i^*) = \sigma(E_i' + \epsilon_{ijk} u_j' B_k') \, , \tag{11}$$

where $(E_i^*)' = E_i' + \epsilon_{ijk} u_j' B_k'$ is the electric field in coordinates moving with the gas velocity u_i' through a magnetic field B_i'. Using the Navier-Stokes aproximation discussed in Sec. 1, and recognizing that the partially ionized plasma is a mixture of monatornic heavy particles (atoms and ions), and an electron gas which can in general maintain distinct temperatures, the heat fluxes and stress tensor can be written

$$q_i' = -\kappa \left(\frac{\partial T'}{\partial x_i'} \right), \quad q_{e,i}' = -\kappa_e \left(\frac{\partial T_e'}{\partial x_i'} \right) \, , \tag{12}$$

$$\tau_{ij}' = -\eta \left(\frac{\partial u_i'}{\partial x_j'} + \frac{\partial u_j'}{\partial x_i'} - \frac{2}{3} \delta_{ij} \cdot \frac{\partial u_k'}{\partial x_k'} \right) , \tag{13}$$

where κ and κ_e are the heavy-particle and electron-gas thermal conductivities and μ is the coefficient of shear viscosity for the entire gas. Combining the Maxwell equation for induced magnetic field, Eq. (7), with Ohm's law, Eq. (11), gives an expression for the gas-frame electric field in term of magnetic field derivatives

$$(E_i^*)' = E_i' + \epsilon_{ijk} u_j' B_k' = \frac{\epsilon_{ijk}}{\sigma\mu_o} \cdot \left(\frac{\partial B_k'}{\partial x_j'}\right) . \qquad (14)$$

Eqs. (2) - (14) are applicable within the transition region of Fig. 1. It is useful to re-express the governing equations in terms of new "unprimed" variables which have been nondimensionalized with respect to quantities in front of the shock. Define:

$$\rho \equiv \frac{\rho'}{\rho_1'} , \quad T \equiv \frac{T'}{T_1'} , \quad T_e \equiv \frac{T_e'}{T_1'} , \quad \Theta_{ion} \equiv \frac{\Theta_{ion}'}{T_1'} \qquad (15)$$

$$x_i \equiv \frac{x_i'}{\lambda_1} , \quad u_i \equiv \frac{u_i'}{u_{x_1}'} , \quad B_i \equiv \frac{B_i'}{B_{x_1}'} , \quad E_i \equiv \frac{E_i'}{u_{x_1}' B_{x_1}'} \qquad (16)$$

$$J_i \equiv \frac{\mu_o \lambda_1 J_i'}{B_{x_1}'} , \quad q_i \equiv \frac{q_i'}{\rho_1' u_{x_1}' R T_1'} , \quad q_{e,i} \equiv \frac{q_{e,i}'}{\rho_1' u_{x_1}' R T_1'} , \qquad (17)$$

$$\tau_{ij} \equiv \frac{\tau_{ij}'}{\rho_1' u_{x_1}'^2} , \qquad (18)$$

where the relationship between tensor indices and the components of Fig. 1 has been discussed. Note also that the subscript 1 in Eqs. (15) - (18) denotes upstream conditions generally, and that λ_1, is the mean free path in the undisturbed gas.

Acoustic and Alfvén speeds a_1' and b_{x1}' are defined which are characteristic of the undisturbed ($\alpha_1 = 0$) state:

$$a_1' \equiv \left(\frac{5}{3} RT_1'\right)^{\frac{1}{2}} , \quad b_{x1}' \equiv B_{x1}' \left(\rho_1' u_o\right)^{-\frac{1}{2}} . \tag{19a}$$

These, in turn, may be used to define the Mach and Alfvén numbers of the shock M_1 and M_{A1}:

$$M_1 \equiv \frac{u_{x1}'}{a_1'} = \frac{u_{x1}'}{\left(\frac{5}{3} RT_1'\right)^{\frac{1}{2}}} , \quad M_{A1} \equiv \frac{u_{x1}'}{b_{x1}'} = \frac{\left(\rho_1' u_{x1}'^2 \mu_o\right)^{\frac{1}{2}}}{B_{x1}'} . \tag{19b}$$

In order to assess the relative significance of viscosity verses electrical conductivity as dissipative mechanisms these transport properties must be incorporated into suitable dimensionless numbers, i.e., fluid dynamic and magnetic Reynolds numbers Re and Rm. Noting that the characteristic length scale in the present problem is the upstream mean free path λ_1, define:

$$Re \equiv \frac{\rho' u_{x1}' \lambda_1}{\eta} , \tag{20}$$

$$Rm \equiv \sigma \mu_o u_{x1}' \lambda_1 ; \tag{21}$$

furthermore, a Prandtl number Pr is defined which incorporates the effects of heavy-particle thermal conductivity,

$$Pr \equiv \frac{5}{2} \cdot \frac{R_\eta}{\kappa} \cdot \qquad (22)$$

It is noted in passing that, from kinetic theory, in a pure monatomic gas $\kappa = (15\, R\eta)/4$, so that when $\alpha = 0$, $Pr = 2/3$.

The governing equations, Eqs. (4) - (14) can now be written in terms of the dimensionless quanties defined by Eqs. (15) - (22) as follows:

$$\frac{\partial}{\partial x_i}(\rho u_i) = \frac{\partial E_i}{\partial x_i} = \frac{\partial B_i}{\partial x_i} = \varepsilon_{ijk} \cdot \frac{\partial E_k}{\partial x_j} = 0 ,$$

$$\frac{\partial}{\partial x_i}\left[\rho u_i u_j + \frac{3}{5M_1^2} \cdot \rho (T + \alpha T_e)\, \delta_{ij} + \frac{1}{M^2_{A_1}} \left(\delta_{ij} \frac{B^2}{2} - B_i B_j\right) + \tau_{ij}\right] = 0 ,$$

$$\frac{\partial}{\partial x_i}\left[\rho u_i \cdot \frac{5}{2}(T + \alpha T_e + \frac{2}{5}\, \alpha \Theta_{ion}) + \frac{5}{6} M_1^2 u^2 \right.$$

$$\left. + \varepsilon_{ijk} \cdot \frac{5}{3} \frac{M_1}{M_{A_1}^2} \cdot E_j B_k + \frac{5}{3} M_1^2 u_j \tau_{ij} + q_i + q_{e,i}\right] = 0,$$

$$E_i + \varepsilon_{ijk} u_j B_k = \frac{J_i}{Rm} = \frac{\varepsilon_{ijk}}{Rm} \cdot \frac{\partial B_k}{\partial x_j} ,$$

$$q_i = -\frac{5}{2} \cdot \frac{1}{Pr\, Re} \cdot \frac{\partial T}{\partial x_i} , \quad q_{e,i} = -\frac{5}{2}\left(\frac{\kappa_e}{\kappa}\right) \cdot \frac{1}{Pr\, Re} \cdot \frac{\partial T_e}{\partial x_i} ,$$

$$\tau_{ij} = \frac{1}{Re}\left[\frac{\partial u_i}{\partial x_j} + \frac{\partial u_j}{\partial x_i} - \frac{2}{3}\delta_{ij}\frac{\partial u_k}{\partial x_k}\right]$$

Bearing in mind the relationship between the tensor notation indices and the components of the vector quantities in Fig. 1, and substituting these quantities into the above set gives the ordinary differential equations:

$$\frac{d}{dx}(\rho u_x) = \frac{dB_x}{dx} = \frac{dE_y}{dx} = 0, \qquad (23)$$

$$\frac{d}{dx}\left[\rho u_x^2 + \frac{3}{5M_1^2}\cdot\rho(T + \alpha T_e) + \frac{1}{2M_{A_1}^2}(B_z^2 - B_x^2) + \tau_{xx}\right] = 0 \qquad (24)$$

$$\frac{d}{dx}\left[\rho u_x u_z - \frac{B_x B_z}{M_{A1}^2} + \tau_{xz}\right] = 0 \qquad (25)$$

$$\frac{d}{dx}\left[\rho u_x \cdot \frac{5}{2}(T + \alpha T_e + \frac{2}{5}\alpha\omega_{ion}) + \frac{5}{6}M_1^2(u_x^2 + u_z^2)\right.$$

$$\left. + \frac{5}{3}\cdot\frac{M_1^2}{M_{A1}^2}\cdot E_y B_z + \frac{5}{3}M_1^2(u_x\tau_{xx} + u_z\tau_{xz}) + q_x + q_{e,i}\right] = 0 \qquad (26)$$

$$\frac{dB_z}{dx} = -J_y = Rm\left[u_x B_z - u_z B_x - E_y\right] , \tag{27}$$

$$q_x = -\frac{5}{2}\cdot\frac{1}{PrRe}\cdot\frac{dT}{dx} , \quad q_{e,i} = -\frac{5}{2}\left(\frac{\kappa_e}{\kappa}\right)\frac{1}{PrRe}\cdot\frac{dT_e}{dx} , \tag{28}$$

$$\tau_{xx} = -\frac{4}{3}\cdot\frac{1}{Re}\cdot\frac{du_x}{dx} , \quad \tau_{xz} = -\frac{1}{Re}\cdot\frac{du_z}{dx} . \tag{29}$$

Eqs. (23) - (26) can be integrated immediately between conditions in the undisturbed gas and some arbitrary point x in the shock interior. Note first that, using the definitions of Eqs. (15) and (16), the flow variables must satisfy the following conditions asymptotically upstream

$$\begin{aligned} @\, x \longrightarrow -\infty \;:\; & u_x = B_x = T = \rho = 1 , \\ & \alpha = u_z = 0 , \quad B_z = B_{z_1} , \quad E_y = E_{y1} . \end{aligned} \tag{30}$$

Now, substituting the fluxes of Eqs. (28) and (29) into Eqs. (24) - (26), and performing the aforementioned integrations with the boundary conditions of Eq. (30), Eqs. (23) - (27) become:

$$\rho u_x = B_x = 1, \quad E_y = E_{y1} \tag{31}$$

$$\frac{du_x}{dx} = \frac{3}{4}\,Re\left[u_x - 1 + \frac{3}{5M_1^2}\left(\frac{T + \alpha T_e}{u_x} - 1\right) + \frac{1}{2M_{A_1}^2}\left(B_z^2 - B_{z_1}^2\right)\right] \tag{32}$$

$$\frac{du_z}{dx} = R_e \left[u_z - \frac{(B_z - B_{z_1})}{M_{A_1}^2} \right], \qquad (33)$$

$$\frac{dT}{dx} = -\left(\frac{\nu_e}{\nu}\right)\frac{dT_e}{dx} - \frac{2}{3} PrM_1^2 \left(\frac{4}{3} u_x \frac{du_x}{dx} + u_z \frac{du_z}{dx}\right)$$

$$+ Pr\,Re \left[T + \gamma T_e + \frac{2}{5} \alpha \omega_{ion} - \Gamma + \frac{M_i^2}{3} (u_x^2 + u_z^2 - 1) \right.$$

$$\left. + \frac{2}{3} \cdot \frac{M_i^2}{M_{A_1}^2} \cdot E_{y_1} (B_z - B_{z_1}) \right] \qquad (34)$$

$$\frac{dB_z}{dx} = Rm \left[B_z \left(u_x - \frac{1}{M_{A_1}^2}\right) + \frac{B_{z_1}}{M_{A_1}^2} - E_y \right] - \frac{Rm}{Re} \cdot \frac{du_z}{dx} \qquad (35)$$

It is instructive to examine, at this point, the significance of the hydromagnetic boundary condition on the electric field E_{y_1}. If the boundary conditions of Eq. (30) are introduced into Eqs. (32) - (34), the flow derivatives quite properly vanish identically in the undisturbed gas:

$$@\, x \longrightarrow -\infty : \frac{du_x}{dx} = \frac{du_z}{dx} = \frac{dT}{dx} = 0$$

In order to insure that the transverse magnetic field vanishes upstream, i.e., $@\, x \longrightarrow -\infty : dB_z/dx = 0$, it is required, from Eqs. (30) and (35), that

$$@x \to -\infty \quad Rm(B_{z_1} - E_{y_1}) = 0 \,. \tag{36}$$

In a pure hydromagnetic discontinuity where the gas is electrically conducting upstream, $Rm_1 \neq 0$, so that from Eq. (36) $E_{y_1} = B_{z_1}$. On the other hand, for the gas-ionizing shocks, of interest here, $\alpha_1 = Rm_1 = 0$, so that E_{y_1} is not uniquely defined.

Eqs. (32)-(35) are four differential equations in the six unknowns: u_x, u_z, B_z, T, T_e and α. In order to mathematically close the set, two additional equations are required describing the nonequilibrium behavior of α and T_e within the shock transition; also the transport-property-dependent dimensionless numbers Re, Rm and Pr must be expressed in terms of local values of the flow variables.

3. IONIZATION RATES AND TRANSPORT PROPERTIES IN PARTIALLY IONIZED ARGON

Formulation of equations which deal specifically with distinct electron, atom and ion species is facilitated by introducing the following approximations, definitions and derived relations, most of which follow directly from the assumptions of Sec. 1:

$$m_e/m_A << 1 \, , \; m_I = m_A \, , \; n_e' = n_I' \, , \; \dot{n}_e' = \dot{n}_I' = -\dot{n}_A' \, , \tag{37}$$

$$\alpha \equiv \frac{n_e'}{n_e' + n_A'} \, , \; \dot{n}_e' = n_e \left(\frac{\dot{\alpha}'}{\alpha}\right) \, , \; n' = 2n_e' + n_A' \, , \tag{38}$$

$$n_e' = \left(\frac{\alpha}{1+\alpha}\right) n' = \frac{\alpha \rho'}{m_A} \, , \; n_A' = \left(\frac{1-\alpha}{1+\alpha}\right) n' = \frac{(1-\alpha)\rho'}{m_A} \, , \tag{39}$$

$$\rho'(1+\alpha) = n' m_A \, , \; \frac{n_e' m_e}{\rho'} = \left(\frac{m_e}{m_A}\right) \alpha \, , \; \frac{n_I' m_I}{\rho'} = \alpha \, , \tag{40}$$

where n_A', n_e' and n_I' are the number densities of Ar, e^- and Ar^+ species respectively, n' is the total number density, $\dot{n}_e'$ is the net electron number density production rate from all sources, $\dot{\alpha}'$ is the degree of ionization production rate from all sources, $m_e = 9.107 \times 10^{-31}$ kg and $m_A = 6.628 \times 10^{-26}$ kg are the masses of an electron and an argon atom, respectively.

The one-dimensional conservation of electron mass and energy equations

applicable to the present problem can be written[26]

$$\frac{d}{dx'}\left(n_e' u_x'\right) = \left(\dot{n}_e'\right)_A + \left(\dot{n}_e'\right)_e \quad , \tag{41}$$

$$n_e' u_x' \cdot \frac{d}{dx'}\left(\frac{3}{2} k T_e'\right) + n_e' k T_e' \cdot \frac{du_x'}{dx'}$$

$$= 3 n_e' \left(\frac{m_e}{m_A}\right) \nu_e' k \left(T' - T_e'\right) - \left(\dot{n}_e'\right)_e k \Theta_{ion}' + \frac{J'^2}{\sigma} \quad , \tag{42}$$

where $k = 1.380 \times 10^{-23}$ Joule/^{o}K is Boltzmann's constant. $\left(\dot{n}_e'\right)_A$ and $\left(\dot{n}_e'\right)_e$ are the electron density production rates resulting from atom-catalyzed reactions Eq. (1a), and electron-catalyzed reactions, Eq. (1b), respectively, and ν_e' is the collision frequency of the electron gas. The effects of electron thermal conductivity were not included in Eq. (42) in anticipation of a future development, however, a Joule heating term J'^2/σ was added to the energy equation of Ref. 26 to account for dissipation due to induced currents flowing through the gas within the transition region.

Making use of Eqs. (4), (38) and (39), and the fact that $R=k/m_A$, Eqs. (41) and (42), in terms of the degree of ionization α, become

$$u_x' \frac{d\alpha}{dx'} = \dot{\alpha}_A' + \dot{\alpha}_e' \quad , \tag{43}$$

$$\frac{3}{2} u_x' \cdot \frac{dT_e'}{dx'} + T_e' \cdot \frac{du_x'}{dx} =$$

$$= 3\left(\frac{m_e}{m_A}\right) \nu_e' \, (T' - T_e') - \frac{\dot{\alpha}_e'}{\alpha} \, \Theta_{ion}' + \frac{1}{\alpha \rho' R} \cdot \frac{J'^2}{\sigma} \,. \qquad (44)$$

The collisional ionization source terms for atom-catalyzed and electron-catalyzed reactions, $\dot{\alpha}_A'$ and $\dot{\alpha}_e'$ respectively, can be expressed[26]

$$\dot{\alpha}_A' = (1 - \alpha)\left(\frac{\rho'}{m_A}\right)^2 \cdot k_{r_A}(T') \cdot \left[\frac{\alpha_{eq}^2(T') - \alpha^2}{1 - \alpha_{eq}^2(T')}\right] , \qquad (45a)$$

$$\dot{\alpha}_e' = \alpha\left(\frac{\rho'}{m_A}\right)^2 \cdot k_{r_e}(T_e') \cdot \left[\frac{\alpha_{eq}^2(T_e') - \alpha^2}{1 - \alpha_{eq}^2(T_e')}\right] , \qquad (45b)$$

where $\alpha_{eq}(T')$ and $\alpha_{eq}(T_e')$ are reference degrees of ionization which would prevail at a given gas density ρ', degree of ionization α and either the heavy-particle temperature T' or the electron temperature T_e'. These, in turn, are defined by:

$$\alpha_{eq}(T') \equiv \left[1 + \frac{\rho'(1 + \alpha)}{m_A K_{eq}(T')}\right]^{-\frac{1}{2}} , \qquad (46a)$$

$$\alpha_{eq}(T_e') \equiv \left[1 + \frac{\rho'(1 + \alpha)}{m_A K_{eq}(T_e')}\right]^{-\frac{1}{2}} , \qquad (46b)$$

where $K_{eq}(T')$ and $K_{eq}(T_e')$ are equilibrium "constants" associated with the heavy-particle and electron temperatures, respectively. The recombination

rate coefficients, $k_{r_A}(T')$ and $k_{r_e}(T_e')$, and equilibrium constants associated with Eqs. (1a, b) behind strong normal shocks, as discussed in Ref. 26, are:

$$k_{r_A}(T') = 5.80 \times 10^{-49} \cdot \left(\frac{135,300}{T'} + 2\right) \cdot \exp\left(\frac{47,800}{T'}\right) \ (m^6/sec), \qquad (47a)$$

$$k_{r_e}(T_e') = 1.29 \times 10^{-44} \cdot \left(\frac{135,300}{T_e'} + 2\right) \cdot \exp\left(\frac{47,800}{T_e'}\right) \ (m^6/sec), \qquad (47b)$$

$$K_{eq}(T') = 2.90 \times 10^{22} \cdot T'^{3/2} \cdot \exp\left(-\frac{\Theta_{ion}'}{T'}\right) \ (1/m^3), \qquad (48a)$$

$$K_{eq}(T_e') = 2.90 \times 10^{22} \cdot T_e'^{3/2} \cdot \exp\left(-\frac{\Theta_{ion}'}{T_e'}\right) \ (1/m^3). \qquad (48b)$$

It is convienient to define nondimensionalized "unprimed" variables $\dot{\alpha}_A$, $\dot{\alpha}_e$, ν_e corresponding to the production rates and collision frequencies appearing in Eqs. (43) and (44):

$$\dot{\alpha}_A \equiv \frac{\lambda_1 \dot{\alpha}_A'}{u_{x_1}'}, \quad \dot{\alpha}_e \equiv \frac{\lambda_1 \dot{\alpha}_e'}{u_{x_1}'} \qquad (49)$$

$$\nu_e \equiv \left(\frac{m_e}{m_A}\right) \frac{\lambda_1 \nu_e'}{u_{x_1}'} \qquad (50)$$

The production rates of Eq. (49) are completely specified in terms of local values of n, T' and T_e' by Eqs. (45a) though (48b). Relations are now sought which express ν_e and also the dimensionless numbers Re, Rm and Pr in terms of n, T' and T_e'.

In principle, all collision-dependent transport properties needed in this analysis are obtainable from a knowledge of the elastic collision cross section for the various encounters occuring in a partially ionized gas. These will be briefly summarized for argon.

The Coulomb cross-sections for collisions between charged particles are[31]

$$Q_{II}' = \frac{e^4}{36\pi(\epsilon_o k T')^2} \cdot \ell n \left[12\pi \cdot \left(\frac{\epsilon_o^3 k^3 T'^3}{e^6 n_e'} \right)^{\frac{1}{2}} \right],$$

$$Q_{eI}' = Q_{ee}' = \frac{e^4}{36\pi(\epsilon_o k T_e')^2} \cdot \ell n \left[12\pi \cdot \left(\frac{\epsilon_o^3 k^3 T_e'^3}{e^6 n_e'} \right)^{\frac{1}{2}} \right],$$

where Q_{II}', Q_{eI}' and Q_{ee}' are the cross-sections for $Ar^+ - Ar^+$, $e^- - Ar^+$ and $e^- - e^-$ collisions respectively, $e = 1.602 \times 10^{-19}$ coulomb is the charge of an electron and $\epsilon_o = 8.854 \times 10^{-12}$ farad/m is the dielectric permittivity of free space in mks units. Making the required numerical substitutions in the above yields

$$Q_{II}' = \frac{1.95 \times 10^{-10}}{T'^2} \cdot \ell n \left[1.53 \times 10^{14} \cdot \frac{T'^3}{n_e'} \right] (m^2), \quad (51a)$$

$$Q_{eI}' = Q_{ee} = \frac{1.95 \times 10^{-10}}{T_e'^{\,2}} \cdot \ln\left[1.53 \times 10^{14} \cdot \frac{T_e'^{\,3}}{n_e'}\right] \quad (m^3) ; \qquad (51b)$$

the remaining cross-sections can be expressed, after Jaffrin[30]:

$$Q_{AA}' = 170 \times 10^{-20} \cdot T'^{-\frac{1}{4}} \quad (m^2) , \qquad (51c)$$

$$Q_{IA}' = 140 \times 10^{-20} \quad (m^2) , \qquad (51d)$$

$$Q_{eA}' = \left\{ \begin{array}{l} (-0.35 + 0.775 \times 10^{-4} \cdot T_e') \times 10^{-20}, \; T_e' > 10^{4o}K \\ (0.39 - 0.551 \times 10^{-4} \cdot T_e' + 0.595 \times 10^{-8} \cdot T_e'^{\,2}) \times 10^{-20}, \; T_e' < 10^{4o}K \end{array} \right\} (m^2), \qquad (51e)$$

where Q_{AA}', Q_{IA}' and Q_{eA}' are the elastic cross-section for Ar - Ar, Ar^+ - Ar and e^- - Ar collisions, respectively.

The electron elastic collision frequency ν_e' and the electrical conductivity of the partially ionized gas σ can be written directly in terms of these cross sections

$$\nu_e' = \left(\frac{8kT_e'}{\pi m_e}\right)^{\frac{1}{2}} (n_A' Q_{eA}' + n_e' Q_{eI}') , \qquad (52)$$

$$\sigma = \frac{e^2 n_e'}{m_e \nu_e'} = \left(\frac{\pi e^4}{8 m_e k T_e'}\right)^{\frac{1}{2}} \frac{n_e'}{n_A' Q_{eA}' + n_e' Q_{eI}'} ; \qquad (53)$$

moreover, the thermal conductivities of the atom, ion and electron species are[30]

$$\varkappa_A = \frac{75k}{64Q_{AA}'}\left(\frac{\pi k T'}{m_A}\right)^{\frac{1}{2}}\left[1 + \frac{n_e' Q_{IA}'}{n_A' Q_{AA}'}\right]^{-1}, \tag{54}$$

$$\varkappa_I = \frac{75k}{64Q_{IA}'}\cdot\frac{n_e'}{n_A'}\cdot\left(\frac{\pi k T}{m_A}\right)^{\frac{1}{2}}\left[1 + \frac{n_e' Q_{II}'}{n_A' Q_{IA}'}\right]^{-1}, \tag{55}$$

$$\varkappa_e = \frac{75\,k}{64Q_{ee}'(1+\sqrt{2})}\cdot\left(\frac{\pi k T_e'}{m_e}\right)^{\frac{1}{2}}\left[1 + \frac{\sqrt{2}\, n_A' Q_{eA}'}{(1+\sqrt{2})\, n_e' Q_{ee}'}\right]^{-1}. \tag{56}$$

The viscosity coefficients are related to the thermal conductivities by

$$\eta_A = \frac{4}{15\,R}\varkappa_A, \quad \eta_I = \frac{4}{15\,R}\varkappa_I, \quad \eta_e = \frac{4}{15R}\left(\frac{m_e}{m_A}\right)\varkappa_e. \tag{57}$$

The upstream mean free path λ_1 which is used here as a reference length is

$$\lambda_1 = \frac{1}{\sqrt{2}\, n_1' Q_{AA1}'} = \frac{m_A}{\sqrt{2}\,\rho_1' Q_{AA1}'}, \tag{58}$$

where Q_{AA1} is Eq. (51c) evaluated at $T' = T_1'$. Note also that

$$\varkappa \equiv \varkappa_A + \varkappa_I, \quad \eta \cong \eta_A + \eta_I; \tag{59}$$

where the electron viscosity has been dropped from η since η_e / η is of the order $(m_e/m_A)^{\frac{1}{2}} \ll 1$; cf. Eqs. (56) and (57).

Combining Eqs. (20), (39), (54), (55), (56), (58) and (59) and introducing the definition of the upstream Mach number $M_1 = u_{x_1}' / (5RT_1')^{\frac{1}{2}}$ gives an expression for the fluid dynamic Reynold's number in terms of α and T:

$$R_e = \left(\frac{128}{15\pi}\right)^{\frac{1}{2}} M_1 T^{-1} \cdot \frac{1}{Q'_{AA_1}} \left[\frac{1-\alpha}{Q'_{AA} + \alpha(Q'_{IA} - Q'_{AA})} + \frac{\alpha}{Q'_{IA} + \alpha(Q'_{II} - Q'_{IA})} \right]^{-1} . \tag{60a}$$

Using the fact that $Q'_{AA} / Q'_{AA_1} = (T'/T_1')^{-\frac{1}{4}} = T^{-\frac{1}{4}}$, from Eq. (51c), Eq. (60) can be simplified considerably if the argon remains un-ionized;

$$@\ \alpha = 0 : \quad R_e = \left(\frac{128}{15\pi}\right)^{\frac{1}{2}} M_1 T^{-3/4} \tag{60b}$$

Combining Eqs. (21), (39), (53) and (58), and using the Mach number, as before, gives an expression for magnetic Reynolds number in terms of α and T_e :

$$Rm = \rho^* M_1 \alpha T_e^{-\frac{1}{2}} \cdot \left[\frac{Q'_{AA1}}{Q'_{eA} + \alpha(Q'_{eI} - Q'_{eA})} \right] , \tag{61a}$$

where ρ^* is a nondimensionalized reference density defined by

$$\rho^* \equiv \frac{\mu_o e^2 \left(\frac{5\pi}{48}\right)^{\frac{1}{2}} \left(\frac{m_e}{m_A}\right)^{\frac{1}{2}}}{\rho_1' Q'^2_{AA1}} = \frac{8.39 \times 10^{-40}}{\rho_1' Q'^2_{AA1}} . \tag{61b}$$

It may be noted here that while the fluid dynamic Reynold's number based on mean free path Re is density - independent, this is not the case for the Magnetic Reynolds number Rm. From Eq. (61) it follows that ρ^* and therefore Rm increase with decreasing upstream density ρ_1' .

Combining Eqs. (39), (50) (52) and (58) with the definition of Mach number gives the following expression for nondimensionalized electron collision frequency in terms of α and T_e :

$$\nu_e = \left(\frac{m_e}{m_A}\right)^{\frac{1}{2}} \left(\frac{12}{5\Gamma}\right)^{\frac{1}{2}} \frac{T_e^{\frac{1}{2}}}{M_1} \cdot \left[\frac{Q_{eA}' + \alpha(Q_{eI}' - Q_{eA}')}{Q_{AA_1}'}\right] \quad . \quad (62)$$

From Eqs. (22), (57) and (59) the Prandtl number of the Mixture is simply

$$Pr = \frac{2}{3} \quad . \quad (63)$$

The conservation of mass and energy equations for the electron gas can be put in a dimensionless form consistent with that of the global conservation equations of Eqs. (32) - (35). Note first from Eqs. (17), (21) and (27). That the term J'^2/σ can be written

$$\frac{J'^2}{\sigma} = \frac{Rm B_{x_1}'^2 u_{x_1}'}{\mu_0 \lambda_1} (u_x B_z - u_z B_x - E_y)^2 \quad . \quad (64)$$

Substituting Eq. (64), together with the dimensionless production rates and collision frequencies of Eqs. (49) and (50) and the unprimed variables defined

earlier by Eqs. (15) - (19), into Eqs. (43) and (44) yields[32]

$$\frac{d\alpha}{dx} = \frac{\dot{\alpha}_A + \dot{\alpha}_e}{u_x} , \tag{65}$$

$$\frac{dT_e}{dx} = \frac{2\nu_e (T - T_e)}{u_x} - \frac{2}{3}\left(\frac{\dot{\alpha}_e}{\alpha}\right)\frac{q_{ion}}{u_x} + \frac{10}{9}\left(\frac{Rm}{\alpha}\right)(u_x B_z - u_z B_x - E_y)^2 . \tag{66}$$

It is significant that Eq. (66) is not singular when $\alpha = 0$ since from Eqs. (45b), (49), (61) and (62) it follows that ν_e, $(\dot{\alpha}_e/\alpha)$ and (R_m/α) are all bounded as $\alpha \longrightarrow 0$. Certain formulations of the electron energy equation which have appeared in the literature have not had this useful and physically reasonable property.

4. INTEGRAL CURVES IN THE "ZND" APPROXIMATION

Equations (32) - (35), (65) and (66), together with the auxiliary algebraic expressions for Re, Rm, Pr, $\dot{\alpha}_A$, $\dot{\alpha}_e$ and ν_e developed in the preceeding section, form a mathematically closed set of six ordinary differential equations in the six primary variables u_x, u_z, B_z, T, T_e and σ. The formal solution of these equations as an initial-value problem starting from the upstream boundary conditions of Eq. (30) is not possible however owing to the mathematical nature of the system. Briefly, this can be explained as follows. The leading edge of the gas-ionizing front must begin as an ordinary hydrodynamic shock, but a predominant characteristic of the Navier-Stokes hydrodynamic shock structure in a monatomic ($Pr = 2/3$) gas is that the integral curve solution in (u_x, T) phase space has a singularity of the node type at the upstream state; consequently, the downstream state is "unattainable" from the upstream state by numerical integration[33]. Since the gas-ionizing shock begins its upstream structural development as a pure gasdynamic shock, the latter conclusion applies to the present case as well.

Fortunately, it is appropriate to employ a useful approximation here which has been developed in the theory of detonation waves. Commonly known as the Zeldovich-von Neumann-Döring (ZND) approximation, in the present context this amounts to recognizing that ionizing reactions of Eqs. (1a,b) are sufficiently "slow" such that gas-ionizing shock structure can be computed in two distinct regions: (1) a perfect-gas viscous shock wave standing in front of (2) a much longer ionization relaxation zone where finite-rate chemistry and hydromagnetic interactions are significant.

It has been recognized, e.g., by Germain[22], Bleviss[24] and Leonard[18], that, for hydromagnetic shocks, when the magnetic Reynold's number is small

compared to the viscous Reynolds number, a viscous shock is imbedded in a much wider region of hydrom. netic interaction. For the (collisionally ionizing) gas-ionizing hydromagnetic waves treated in the present paper, this must be the case since realistic ionization rate-processes yield values of $Rm/Re \ll 1$ within the initiating perfect-gas shock regardless of the ultimate electrical conductivity level[34]. It should also be clearly understood that unlike certain imbedded viscous shocks which can occur in pure hydromagnetic wave fronts, the imbedded shock here must stand upstream of the hydromagnetic interaction since it creates the necessary electrically conducting environment.

The equations governing flow in the two regions can be obtained formally from Eqs. (32)-(35), (65) and (66) by applying the appropriate limiting conditions. In the perfect-gas-shock region we have the limit: $\alpha \to 0$, $Rm \to 0$, so that Eqs. (65) and (66) for α and T_e are not relevant and Eqs. (30), (32)-(35) become

$$\frac{du_z}{dx} = 0 \ , \ u_z = u_{z_1} = 0 \ ; \ \frac{dB_z}{dx} = 0 \ , \ B_z = B_{z_1} \ ; \tag{66}$$

$$\frac{du_x}{dx} = \frac{3}{4} \ Re \left[u_x - 1 + \frac{3}{5M_1^2} \left(\frac{T}{u_x} - 1 \right) \right] \ , \tag{67}$$

$$\frac{dT}{dx} = - \frac{16}{27} M_1^2 \ u_x \frac{du_x}{dx} + \frac{2}{3} \ Re \left[T - 1 + \frac{M_1^2}{3} \left(u_x^2 - 1 \right) \right] \ , \tag{68}$$

where we have used the fact that $Pr = 2/3$ in the above. Clearly the transverse magnetic field and transverse velocity are constant across the perfect-gas shock. Eqs. (67) - (68) describe the Navier-Stokes shock structure of a perfect monatomic gas. Their solution has been treated elsewhere[35-37], and is discussed here in the Appendix. The upstream and downstream states implied by these equations can be found by setting $du_x / dx = dT/dx = 0$ in Eqs. (67) and (68),

$$u_x - 1 + \frac{3}{5M_1^2}\left(\frac{T}{u_x} - 1\right) = 0\,, \quad T - 1 + \frac{M_1^2}{3}\left(u_x^2 - 1\right) = 0,$$

eliminating the temperature T between these to get the quadratic

$$4u_x^2 - \left(5 + \frac{3}{M_1^2}\right) u_x + \left(1 + \frac{3}{M_1^2}\right) = 0,$$

and solving for the velocities and corresponding temperatures associated with the two roots. This yields the upstream and downstream states of the imbedded perfect-gas shock:

$$@x \longrightarrow -\infty\,; \quad u_x = T = 1\,, \tag{69a}$$

$$@x \longrightarrow +\infty\,; \quad u_x = \frac{1}{4}\left(1 + \frac{3}{M_1^2}\right)\,, \quad T = \frac{5}{16}\left(M_1^2 - \frac{3}{5M_1^2}\right) + \frac{7}{8}\,. \tag{69b}$$

In the relaxation zone regions the governing equations are found by applying the limit $Re \longrightarrow \infty$ to Eqs. (32) - (35) which yields the set

$$u_x - 1 + \frac{3}{5M_1^2}\left(\frac{T + \alpha T_e}{u_x} - 1\right) + \frac{1}{2M_{A_1}^2}(B_z^2 - B_{z1}^2) = 0, \qquad (70)$$

$$u_z = \frac{B_z - B_{z1}}{M_{A1}^2}, \qquad (71)$$

$$T + \alpha T_e + \frac{2}{5}\alpha\Theta_{ion} - 1 + \frac{M_1^2}{3}(u_x^2 - 1)$$

$$+ \frac{2}{3} \cdot \frac{M_1^2}{M_{A1}^2} \cdot (B_z - B_{z1})\left(E_y + \frac{B_z - B_{z1}}{2M_{A1}^2}\right) = 0, \qquad (72)$$

$$\frac{dB_z}{dx} = Rm\left[B_z\left(u_x - \frac{1}{M_{A1}^2}\right) + \frac{B_{z1}}{M_{A1}^2} - E_{y1}\right] \equiv Rm \cdot g(u_x, B_z) \qquad (73)$$

Eliminating the quantity $(T + \alpha T_e)$ between Eqs. (70) and (72) gives a quadratic equation in u_x corresponding to $Re \longrightarrow \infty$,

$$f(u_x, B_z, \alpha) \equiv 4u_x^2 - \left(5 + \frac{3}{M_1^2} + \epsilon_1\right)u_x + \left(1 + \frac{3}{M_1^2} - \epsilon_2\right) = 0, \qquad (74)$$

where $$\epsilon_1 \equiv -\frac{5}{2} \cdot \frac{B_z^2 - B_{z1}^2}{M_{A1}^2},$$

$$\epsilon_2 = \frac{6}{M_1^2}\left[\frac{1}{5}\,\alpha\theta_{ion} + \frac{1}{3}\cdot\frac{M_1^2}{M_{A1}^2}(B_z - B_{z1})\left(E_{y1} + \frac{B_z - B_{z1}}{2M_{A1}^2}\right)\right].$$

In the ionization relaxation zone the flow will proceed along the path $f = 0$; it is useful to introduce an analogous path, $g = 0$, corresponding to the limit $Rm \to 0$

$$g(u_x, B_z) = B_z\left(u_x - \frac{1}{M_{A1}^2}\right) + \frac{B_{z1}}{M_{A1}^2} - E_{y1} = 0. \qquad (75)$$

Equation (74) has two roots, given by

$$u_x = \frac{1}{8}\left\{5 + \frac{3}{M_1^2} + \epsilon_1 \pm \left[9\left(1 - \frac{1}{M_1^2}\right)^2 + \epsilon_1^2 + \left(10 + \frac{6}{M_1^2}\right)\epsilon_1 + 16\,\epsilon_2\right]^{1/2}\right\}, \qquad (76)$$

while solving for u_x from Eq. (75) gives

$$u_x = \frac{E_{y1}}{B_z} + \frac{1}{M_{A1}^2}\left(1 - \frac{B_{z1}}{B_z}\right). \qquad (77)$$

Prior to discussing numerical shock structure solutions in physical space, it is instructive to examine the path of the ZND solutions in (u_x, B_z) phase space. Since the integral curves are more meaningful if a distinction is made between "fast" and "slow" hydromagnetic waves, these classifications will be briefly reviewed in the context of the present work.

Analysis of the linearized hydromagnetic equations yields the so-called

fast and slow disturbance speeds c_{f_1}' and c_{s_1}' which, together with the acoustic and Alfvén speeds a_1' and b_{x_1}' of Eq. (19a), are properties of the undisturbed flow. These speeds are conveniently written in terms of the quantity

$$b_1' \equiv (b_{x1}'^2 + b_{z1}'^2)^{\frac{1}{2}} = b_{x_1}' \left[1 + \left(\frac{B_{z1}'}{B_{x_1}'}\right)^2\right]^{\frac{1}{2}} = b_{x1}' (1 + B_{z1}^2)^{\frac{1}{2}} \tag{78}$$

as follows:[38]

$$c_{f_1}' = \left[\frac{1}{2}\left\{(a_1'^2 + b_1'^2) + \sqrt{(a_1'^2 + b_1'^2)^2 - 4a_1'^2 b_{x1}'^2}\right\}\right]^{\frac{1}{2}}, \tag{79a}$$

$$c_{s_1}' = \left[\frac{1}{2}\left\{(a_1'^2 + b_1'^2) - \sqrt{(a_1'^2 + b_1'^2)^2 - 4a_1'^2 b_{x1}'^2}\right\}\right]^{\frac{1}{2}}. \tag{79b}$$

Pure hydromagnetic shocks are generally classified as either fast or slow depending on whether they satisfy the inequalities[39]

$$\frac{u_{x1}'}{c_{f_1}'} \geq 1 \; ; \text{ fast shock,} \tag{80a}$$

$$\frac{c_{s_1}'}{b_{x1}'} \leq \frac{u_{x1}'}{b_{x1}'} < 1 \; ; \text{ slow shock.} \tag{80b}$$

Using the definitions $M_1 \equiv u_{x1}'/a_1'$, $M_{A1} \equiv u_{x1}'/b_{x1}'$ and Eq. (78), the following useful formulas are obtained:

$$\frac{u_{x_1}'}{c_{f_1}'} = \left[\frac{1}{2}\left\{\frac{1}{M_1^2} + \frac{1+B_{z_1}^2}{M_{A_1}^2} + \sqrt{\left(\frac{1}{M_1^2} + \frac{1+B_{z_1}^2}{M_{A_1}^2}\right)^2 - \frac{4}{M_1^2 M_{A_1}^2}}\right\}\right]^{-\frac{1}{2}}, \quad (81a)$$

$$\frac{u_{x_1}'}{c_{s_1}'} = \left[\frac{1}{2}\left\{\frac{1}{M_1^2} + \frac{1+B_{z_1}^2}{M_{A_1}^2} - \sqrt{\frac{1}{M_1^2} + \frac{1+B_{z_1}^2}{M_{A_1}^2}^2 - \frac{4}{M_1^2 M_{A_1}^2}}\right. - \right. \quad (81b)$$

For the purposes of this section, attention is restricted to (hydromagnetically) oblique shocks in the infinite Mach number limit, since hypersonic ($M_1 >> 1$) Mach numbers yield ionization levels required for hydromagnetic interaction and this particular limit does not change any important features of the integral curves. For $M_1 \to \infty$ then, Eqs. (81a, b) give $u_{x_1}'/c_{f_1}' = M_{A_1}(1+B_{z_1}^2)^{-1/2}$ and $c_{s_1}'/u_{x_1}' = 0$. For the special case when the upstream magnetic field is inclined at 45° to the shock front ($B_{x_1} = B_{z_1} = 1$), the criteria of Eqs. (80a, b) become

$$\begin{aligned} M_{A_1} &\geq \sqrt{2} \quad : \text{ fast shock,} \\ 0 \leq M_{A_1} &< 1 \quad : \text{ slow shock.} \end{aligned} \quad (82)$$

It might be observed here that no pure hydromagnetic shocks can exist between the weakest (acoustic) fast wave at $M_{A_1} = \sqrt{2}$ and the slowest (switch-off) slow wave at $M_{A_1} = 1$.

Returning to the discussion of integral curves in the ZND approximation, the 45° upstream magnetic field and $M_1 \to \infty$ assumptions (which were introduced to make the problem specific) should be borne in mind as they apply to the balance of this section. From Eqs. (69a, b) one can expect

an initial jump in streamwise velocity from $u_x = 1$ to $u_x = 1/4$ while $B_z = 1$ remains constant, corresponding to the perfect-gas-shock transition. This imbedded shock transition is denoted: $1 - 1^*$, where 1^* is the downstream state of the perfect-gas shock. Subsequently, the flow progresses in the relaxation zone along the path $f(u_x, B_z, \alpha) = 0$, until the downstream state of the gas-ionizing shock is attained. The latter step of the overall shock transition is denoted: $1^* - 2$. As a conseqence of all flow derivatives vanishing downstream, e.g. $du_x/dx = dB_z/dx = 0 \quad @x \longrightarrow \infty$, the downstream state in the (u_x, B_z) plane is indicated by the intersection of the curves $f(u_x, B_z) = 0$ and $g(u_x, B_z) = 0$. Note that in the infinite Mach number case

$$\lim_{M_1 \longrightarrow \infty} \frac{6\alpha\Theta_{ion}}{5 M_1^3} = 0 ,$$

so that, from Eq. (74), $f = f(u_x, B_z)$ does not depend on α.

(a) Fast Shocks

Consider now the possible trajectories of the fast shock $M_{A_1} = \sqrt{10}$ $(>\sqrt{2})$ shown in Fig. 2. Recall from Eq. (36) that because $\alpha_1 = Rm_1 = 0$, an indeterminacy exists in the value of E_{y_1} for gas-ionizing shocks; it is therefore appropriate at this point to treat the shock-frame electric field as a free parameter. This was done in Fig. 2 which shows the curves $f = 0$ and $g = 0$ computed from Eqs. (76) and (77) for (a) $E_{y1} = 1.0$, (b) $E_{y1} = 0.625$ and (c) $E_{y1} = 0.25$. The first trajectory, nam that with $E_{y1} = B_{z1} = 1.0$, corresponds to the upstream boundary condition on the electric field in a pure hydromagnetic shock, cf. Eq. (36). As indicated previously, the transition, if it occurs, must take place by the path $1 - 1^* - 2$ in the ZND model. It can be

shown that this path is impossible for fast shocks from the following argument: Since $g < 0$ below the curve $g = 0$, it follows from Eq. (73) that $dB_z/dx < 0$ at point 1^* ($R_m > 0$, of course); but $B_{z_2} > 1$, from the intersection point of $g = 0$ and $f = 0$; therefore, the downstream state is inaccesible by the path $1^* - 2$ along the $f = 0$ curve since the magnetic induction equation predicts a decrease rather than the required increase in transverse magnetic field. The same reasoning applies for all valves of $E_{y_1} > 1/4$, cf. Fig. 2(b).

An analogous, but oppositely directed situation occurs when $E_{y_1} < 1/4$, since $B_{z_2} < 1$ and the $1 - 1^* - 2$ transition becomes impossible because $g > 0$ along $1^* - 2$ and Eq. (73) predicts an increase of B_z instead of the required decrease. In fact, the only permitted $1 - 1^* - 2$ transition in a fast gas-ionizing shock is the degenerate case of $E_{y_1} = 0.25$ in Fig. 2(c), which is nothing more than a pure gas shock with no change in magnetic field: ($u_{x_2} = 1/4$, $B_{z_2} = B_{z_1} = 1$).

If the gas were electrically conducting upstream, but with $Rm/Re << 1$, the pure hydromagnetic transition $1 - 2$, along the upper branch of the $f = 0$ curve in Fig. 2(a), would be indicated. In this regime $g > 0$, $dB_z/dx > 0$, and there are no contradictions of the type encountered in the ZND gas-ionizing integral curves. As indicated previously, this branch must be ruled out here since it violates the gas-ionizing archetype of Sec. 1.

Although switch-on ($B_{z_1}=0$, $B_{z_2}\neq 0$) and transverse ($B_x = B_{x_1} = 0$) gas-ionizing shocks have not been dealt with specifically, it can be shown that ZND structures are impossible in these shocks, for the same general reasons that were given for the fast oblique shocks discussed in this section.

(b) Slow Shocks

From Fig. 3 it is evident that the $f = 0$ and $g = 0$ curves for slow shocks take substantially different forms from those of the aforementioned fast shocks. These curves are plotted for the slow shock $M_{A_1} = 1/\sqrt{2}$ (<1) at five different values of the shock-frame electric field: (a) $E_{y_1} = 0.25$, (b) $E_{y_1} = 0.625$, (c) $E_{y_1} = 1.0$, (d) $E_{y_1} = 1.50$ and (e) $E_{y_1} = 2.0$. In this case, Fig. 3(c) is the plot associated with the pure hydromagnetic boundary condition on the electric field. All the electric fields shown have in common the property that ZND structures are possible. After the $1 - 1^*$ perfect-gas-shock transition the flow is in a region where $g < 0$; but $B_{z_2} < 1$ in this case so the derivative $dB_z/dx < 0$ [from Eq. (73)] is in the proper direction, thereby permitting the $1 - 1^* - 2$ path to the downstream state. There are two limiting cases of interest: (1) $E_{y_1} = 1/4$ in Fig. 3(a) is the degenerate case corresponding to the pure gasdynamic shock with constant magnetic field and (2) $E_{y_1} = 2.0$ in Fig. 3 (e), which yields a new kind of switch-off shock which can only occur in gas-ionizing fronts. It follows from Eq. (73) that when $E_{y_1} = B_{z1} / M_{A_1}^2 = 2.0$, $g = 0$ along the straight lines $B_z = 0$ and $u_x = 1 / M_{A1}^2 = 2$. The latter part of the $g = 0$ curve is not visible in this plot because the ordinate is cut off at $u_x = 1.2$. Since the intersection of the $f = 0$ curve with $B_z = 0$ corresponds to the downstream state, the lab-frame electric field $E_{y_1} = B_{z_1} / M_{A_1}^2$ results in a complete switch-off of the transverse magnetic field. The switch-off shock is only possible in ordinary hydromagnetics when $M_{A_1} = 1$, but it is clearly obtainable in slow gas-ionizing shock waves propagating at other Alfvén numbers.

5. NONEQUILIBRIUM NUMERICAL SOLUTIONS

It should be clear by this point that the mathematical nature of the problem in the present ZND approximation is fundamentally different from that implied originally by Eqs. (32)-(35), (65), (66) and the associated initial conditions of Eq. (30). Rather than attempt the solution of six differential equations in the major flow variables u_x, u_z, B_z, T, T_e and α, it is proposed instead to solve simpler sets of equations in two different regions and to match their solutions at a suitable point. Specifically, in the perfect-gas-shock region, only two differential equations need be integrated [Eqs. (67) and (68)], while in the ionization relaxation zone there are three [Eqs. (65), (66) and (73)]. In the latter case, the velocity components u_x, u_z and the heavy-particle temperature T are evaluated locally from algebraic relations [Eqs. (71), (72) and (76)]. In addition, the local values of $\dot{\alpha}_A$, $\dot{\alpha}_e$, Rm and ν_e needed to numerically integrate the relaxation zone differential equations are available from relations introduced and developed in Sec. 3 [Eqs. (45a,b), (51b,c,d), (61a,b) and (62)].

In order to solve for the distribution of flow variables within the gas-ionizing front, two different IBM 7090 computer programs were created: one to solve the perfect-gas Navier-Stokes shock structure problem (see Appendix) and the other to solve the hydromagnetic ionization relaxation zone problem. Since the perfect-gas-shock structure extends from $x = -\infty$ to $x = +\infty$ and the ionization relaxation extends from some finite value of x (say x=0) to $x = +\infty$, the two regimes overlap in physical space; consequently, it was necessary to cut the perfect gas shock solution off at some arbitrary point, as explained in the Appendix and tack it on again to the beginning of the relaxation zone in order to construct a single-valued solution

over the entire range of x, from $-\infty$ to $+\infty$. The somewhat legislated nature of this matching procedure is characteristic of so-called singular perturbation problems — these are invariably generated by physical processes which involve disparate length scales — and is a familiar feature of boundary-layer solutions and detonation wave structure solutions in the ZND approximation[40]. It is possible, in principle, to obtain a more rigorous formulation of the connecting region between the two solutions by the method of matched asymptotic expansions[41].

For all calculations discussed in this section it was assumed that the fronts propagate into "cold" un-ionized argon which is at a pressure of $p_1' = 1.0$ mm Hg = 1.33×10^2 newton/m^2 and a temperature of $T_1' = 300^\circ$K and has a corresponding upstream mean free path of $\lambda_1 = 5.38 \times 10^{-5}$m; furthermore, all of these fronts were considered to be traveling at the same gas dynamic Mach number $M_1 = 20$, corresponding to an upstream flow velocity of $u_{x1}' = 6.45 \times 10^3$m/sec, when viewed from a shock-fixed reference frame. It will become evident that a number of phenomena of interest develop at these flow conditions.

Figure 4 shows the results of a combined perfect-gas-shock and relaxation zone calculation for the limiting case of an ordinary hydrodynamic gas-ionizing front, i.e., with no imposed electric or magnetic fields: $E_{y1} = B_{x1} = B_{z1} = 0$. The solutions have been jointed at $x = 0$ and the scale has been stretched by a factor of ten for $x < 0$ compared to $x > 0$ scale in order to show the relatively narrow Navier-Stokes shock structure. Clearly, the ionization relaxation takes place over several hundred upstream mean free paths compared to the few mean free paths required by the perfect-gas shock, thus providing an *á posteriori* verification of the assumptions leading to the ZND approximation. The relaxation zone behavior of a purely hydrodynamic front has been discussed elsewhere[26].

It should be mentioned that the initial electron temperature used here in the numerical integration of Eq. (66) in all cases was taken as $T_e(0) = T(0) = T^*$. Although the value of electron temperature immediately behind the perfect-gas shock is not well defined (since $\alpha = 0$ there), it was shown in Ref. 26 that relaxation zone calculations are almost entirely insensitive to arbitrarily selected initial values of the electron temperature.

For reasons explained in Sec. 4, it is not possible to compute ZND structures for fast gas-ionizing fronts, so attention has been turned toward the family of slow oblique shocks discussed previously, whose upstream magnetic field is inclined at 45° to the front and whose Alfvén number is $M_{A_1} = 1/\sqrt{2}$. In dimensional terms, the corresponding streamwise magnetic field upstream is $B_{x_1} = 0.473$ Wb/m^2, a reasonably attainable value in laboratory experiments. Structure calculations were carried out with various values of the electric field. These results are displayed in Figs. 5 and 6, respectively, for the pure hydromagnetic boundary condition on the electric field $E_{y_1} = 1.0$, and for the gas-ionizing switch-off shock $E_{y_1} = 2.0$, whose somewhat unique existence was discussed earlier in Sec. 4. As the nonequilibrium ionization progresses and the gas becomes electrically conducting the transverse magnetic field is decreased. In the case of Fig. 6 it is completely switched off. The energy associated with the magnetic field is consequently transferred into other modes, i.e., thermal and ionization energy. The converted magnetic energy can be viewed as an effective exothermicity within the front. The scale stretching for $x < 0$ discussed previously was also applied to the plots in Fig. 5 and 6 so that, even though they appear to be approximately the same width, the perfect-gas-shock is still an order of magnitude narrower than the relaxation zone in the extreme case of $E_{y_1} = 2.0$ (Fig. 6).

As indicated in Sec. 1, it has been held by certain writers that the electric field E_{y_1} associated with a gas-ionizing hydromagnetic front will be determined by the structure. On the other hand, it was shown in Sec. 4 that, although structural considerations may well rule out the steady-state existence of certain (fast) gas-ionizing shocks, they do not appear to furnish a criteria as to which of the possible electric fields will actually be observed in the (slow) shocks whose existence, in the ZND approximation, is possible. Fig. 7 illustrates computed distribution of downstream values B_{z_2}, T_2, u_{x_2} and α_2 corresponding to the upstream conditions discussed previously for various values of the shock-frame electric field E_{y_1}. Also shown is a scale indicating the corresponding nondimensionalized lab-frame electric field (which happens to equal the upstream gas-frame electric field $E^*_{y_1} = E_{y_1} - B_{z_1}$, since the undisturbed gas is obviously motionless with respect to the laboratory). Evidently B_{z_2} decreases almost linearly with increasing electric field until it is finally switched-off at $E_{y_1} = 2.0$. It is interesting that $B_{z_2} = 1.0$ occurs at $E_{y_1} \cong 0.1$, rather than $E_{y_1} = 0.25$ as one might expect from Fig. 3(a). This is due to the finite Mach number used in the present calculations, so that $6\,\alpha\,\Theta_{ion}/5M_1^2$ was not zero as assumed in the Fig. 3 plots. As B_{z_2} decreases in Fig. 7, α_2 and T_2 increase as energy is redistributed. Ultimately when the equilibrium gas becomes fully ionized, at about $E_{y_1} = 1.2$, the kinetic energy $u_x^2/2$ and hence u_x increases as well.

The extent of the relaxation zone can be estimated if we define a suitable characteristic length ℓ_r (strictly speaking, of course, equilibrium is not attained until $x \to \infty$). Consistent with Ref. 26, let:

$$\ell_r = [x]_{\alpha=(2)^{-\frac{1}{2}}\,\alpha_2} \tag{83}$$

The upper graph in Fig. 7 shows the variation of this nondimensionalized relaxation length $\ell_r = \ell_r'/\lambda_1$, where ℓ_r' is the physical relaxation length. Since the perfect-gas shock is the same thickness, $\ell_s \cong \ell_s/\lambda_1 = 7$, in all cases (because it depends only on

upstream Mach number) it follows from this plot that $\ell_s/\ell_r \ll 1$ for all values of E_{y_1}, thus justifying the ZND approximation for these particular calculations.

6. CONCLUDING REMARKS

The present study has dealt theoretically with the existence and structure of gas-ionizing hydromagnetic shock waves, as defined by the archetype of Sec. 1. In the case singled out for attention, the gas within the front was collisionally ionizing argon (by atom-atom and electron-atom impacts) in a nonequilibrium two-temperature state. In view of the relatively low temperature expected, photo-ionization was ruled out on an ad hoc basis; moreover, the ionization lags associated with finite-rate chemistry indicated that the ZND approximation could be employed. This model, in turn, led to a number of surprising results: (1) No steady-state structure could be constructed for fast gas-ionizing waves; (2) for the slow waves, where numerical solutions were obtained, the ZND approximation was verified a posteriori for the shock conditions studied here; and (3) the Rankine-Hugoniot indeterminacy of the electric field, which is intrinsic to the concept of gas-ionizing shocks, was not removed by considerations of structure.

As to the applicability and relevance of these results, it should be first recalled that "high temperature" gas-ionizing shocks were ruled out at the outset on the physical grounds that they create radiation-induced electron precursors and hence make the upstream state electrically conducting; but any "gas-ionizing" shock which propagates in the real world must move into a region where there is some electrical conductivity, however small. Consequently, the gas-ionizing archetype actually presupposes some low threshold below which the gas acts as though it were non-electrically-conducting. It is not entirely clear that such a threshold exists physically. Furthermore, even in the supposed low temperature case considered here, the post shock temperatures become sufficiently high (since the slow shock is effectively exothermic) to indicate a relatively high level of precursor ionization, particularly for large electric fields. For this reason, in lieu of specific experimental evidence to the contrary, it seems quite possible that solutions with arbitrarily selected electric fields are not obtained in practice, and that only the solution with a purely

hydromagnetic boundary condition on the elctric field has physical significance.

It is suggested that future research into the nature of hydromagnetic shocks propagating into "cold" upstream states might profitably include the effects of radiative nonequilibrium and photo-ionizing reactions in the analytical models.

FOOTNOTES

1. A.G. Kulikovskii and G.A. Lyubimov, Dokl. Akad. Nauk SSSR 129, 52 (1959) [English transl: Soviet Physics - Doklady 4,1185 (1960)].
2. A.G. Kulikovskii and G.A. Lyubimov, Dokl. Akad. Nauk SSSR 129, 525 (1959) [English transl: Soviet Physics - Doklady 4, 1195 (1960)].
3. A.G. Kulikovskii and G.A. Lyubimov, Rev. Mod. Phys. 32, 977 (1960).
4. G.A. Lyubimov, Dokl. Akad. Nauk SSSR 126, 291 (1959) [English transl: Soviet Phys. - Doklady 4, 510 (1959)].
5. G.A. Lyubimov, Izvestiia Akademii Nauk SSSR, Otdelenie Tedhnicheskikh Nauk, Mechanika i Mashinostroenie 5, 9 (1959) [English transl: ARS J. 30, 416 (1960)].
6. W. Kunkel and R.A. Gross, in Plasma Hydromagnetics, Ed. by D. Bershader (Stanford University Press, Stanford, California, 1962), pp. 58-82.
7. J.B. Helliwell, Phys. Fluids 6, 1516 (1963).
8. C.K. Chu, Phys. Fluids 7, (1964).
9. L.C. Woods, J. Fluid Mech. 22, 689 (1965).
10. R.M. May and J. Tendys, Nuclear Fusion 5, 144 (1965).
11. R.T. Taussig, Phys. Fluids 8, 1616 (1965).
12. R.T. Taussig, Phys. Fluids 9, 421 (1966).
13. R.A. Gross, Rev. Mod. Phys. 37, 724 (1965).
14. J.H. Clarke and C. Ferrari, Phys. Fluids 8, 2121 (1965).
15. F. de Hoffmann and E. Teller, Phys. Rev. 80, 692 (1951).
16. K.O. Friedrichs and H. Kranzer, New York University Report NYO 6486 (1958).
17. J. Bazar and W.B. Ericson, Astrophys. J. 129, 758 (1958).
18. B.P. Leonard, Phys. Fluids 9, 917 (1966).
19. W. Marshall, Proc. Roy. Soc. (London) A 233, 367 (1955).
20. J.M. Burgers, in Magnetohydrodynamics, Ed. by R.K.M. Landshoff (Stanford University Press, Stanford, California, 1957), pp. 36-56.

21. G.S.S. Ludford, J. Fluid Mech. 5, 67 (1959).

22. P. Germain, Rev. Mod. Phys. 32, 951 (1960).

23. P. Germain, Office National d'Etudes et de Researches Aérospatiales (ONERA) T.P. no. 241 (1965).

24. Z.O. Bleviss, J. Fluid Mech. 9, 49 (1960).

25. J.E. Anderson, Magnetohydrodynamic Shock Waves (MIT Press, Cambridge, Massachusetts, 1963).

26. M.I. Hoffert and H. Lien, Phys. Fluids (to be published).

27. J. D. Jukes, J. Fluid Mech. 3, 275 (1957).

28. M.S. Grewal and L. Talbot, J. Fluid Mech. 16, 573 (1963).

29. M.Y. Jaffrin and R.F. Probstein, Phys. Fluids 7, 1658 (1964).

30. M.Y. Jaffrin, Phys. Fluids 8, 606 (1965).

31. G.W. Sutton and A. Sherman, Engineering Magnetohydrodynamics (McGraw-Hill Book Company, New York, 1965), p. 144.

32. The term $(2T_e/3u_x)(dT_e/dx)$ has been dropped here, as in Ref. 26, since it is always negligibly small in shock relaxation zones compared to the other terms in Eq. (66).

33. W.D. Hayes, Gasdynamic Discontinuities (Princeton University Press, Princeton, New Jersey, 1960).

34. This was verified a posteriori for the shock structure calculations presented here.

35. M. Morduchow and P. Libby, J. Aero. Sci. 16, 674 (1949).

36. H. Grad, Commun. on Pure and Applied Math. 5, 257 (1952).

37. D. Gilbarg and D. Paulucci, J. Rat. Mech. Anal. 2, 617 (1953).

38. A. Jeffrey and T. Taniuti, Non-Linear Wave Propagation (Academic Press, New York, 1964) p. 173.

39. Ibid., p. 223.

40. F.A. Williams, Combustion Theory (Addison-Wesley Publishing Company, Inc., Reading, Massachusetts, 1965), p. 150.

41. J.R. Bowen, Phys. Fluids 10, 290 (1967).

APPENDIX - INTEGRATION OF THE NAVIER-STOKES SHOCK STRUCTURE EQUATIONS IN UN-IONIZED ARGON

The numerical solution of the imbedded perfect-gas viscous shock structure, while not entirely straightforward, is well-understood and will be discussed briefly here. The applicable differential equations in u_x and T are [cf. Eqs. (67) and (68)]:

$$\frac{du_x}{dx} = Re \cdot F(u_x, T) \equiv \frac{3}{4} Re \left[u_x - 1 + \frac{3}{5 M_1^2} \left(\frac{T}{u_x} - 1 \right) \right], \qquad (A1)$$

$$\frac{dT}{dx} = Re \cdot G(u_x, T) \equiv - \frac{16}{27} M_1^2 u_x \frac{du_x}{dx}$$

$$+ \frac{2}{3} Re \left[T - 1 + \frac{M_1^2}{3} (u_x^2 - 1) \right]. \qquad (A2)$$

Ordinary, numerical integration of such differential equations as an initial-value problem would be indicated. It is well-known, however, that this is not possible for this particular system because the derivative $dT / du_x = G(u_x, T) / F(u_x, T)$ becomes indeterminate, of the form 0/0, at the upstream and downstream states where $F = G = 0$; moreover, the singular-point is of the node type upstream and of the saddle-point type downstream;

consequently, a stable numerical solution is obtained by integrating from the downstream state toward the upstream, but not vice versa. It might be mentioned that the energy equation has an exact integral for $Pr = 3/4$, in which case singular points in (u_x, T) space are irrelevant to numerical integration[35]. Remember, however, that in the present problem $Pr = 2/3$ so integration must proceed backward from the vicinity of the downstream point.

We can obtain consistent initial values for (u_x, T) in the neighborhood of (u_x^*, T^*), where the asterisk (*) denotes the downstream state of the perfect gas shock, provided we know the value of the derivative asymptotically downstream, viz. $\lim x \longrightarrow \infty \; dT/du_x$. To this end, consider the situation when u_x and T are perturbed slightly an amount Δu_x and ΔT from their downstream values

$$u_x = u_x^* + \Delta u_x , \quad T = T^* + \Delta T ,$$

where $\Delta u_x / u_x^* << 1$, $\Delta T / T^* << 1$. To simplify the algebra, we make the reasonable (for the present problem) assumption that $M_1^2 >> 1$ so that all terms of order $1/M_1^2$ or less compared to unity will henceforth be dropped. The downstream values, from Eq. (69b), become $u_x^* = 1/4$, $T^* = 5M_1^2/16$ and the corresponding near-downstream velocity and temperature are

$$u_x = \frac{1}{4} + \Delta u_x , \quad T = \frac{5}{16} M_1^2 + \Delta T . \tag{A3}$$

Substituting Eq. (A3) into Eqs. (A1) and (A2) and dropping perturbation terms consistent with $\Delta u_x << 1/4$ and $\Delta T << 5M_1^2/16$ yields the linearized equations

$$\frac{du_x}{dx} = \frac{3}{4} R_e \left(\Delta u_x + \frac{12}{5 M_1^2} \cdot \Delta T \right) , \tag{A4}$$

$$\frac{dT}{dx} = - \frac{4}{27} M_1^2 \cdot \frac{du_x}{dx} + \frac{2}{3} R_e \left(\frac{M_1^2}{6} \cdot \Delta u_x + \Delta T \right) . \tag{A5}$$

Dividing (A4) into (A5) gives

$$\frac{dT}{du_x} = - \frac{4}{27} M_1^2 + \frac{\frac{2}{3}\left(\frac{M_1^2}{6} + \frac{\Delta T}{\Delta u_x} \right)}{\frac{3}{4}\left(1 + \frac{12}{5 M_1^2} \cdot \frac{\Delta T}{\Delta u_x} \right)} . \tag{A6}$$

Now, making use of the identities

$$\lim_{x \to \infty} \frac{dT}{du_x} = \lim_{x \to \infty} \frac{\Delta T}{\Delta u_x} = \left(\frac{dT}{du_x} \right)^* ,$$

and evaluating Eq. (A6) at $x \to \infty$ in the above leads to an equation for $(dT/du)^*$ which is exact at the downstream singular-point (accepting, of course, the approximations related to $1/M_1^2 \ll 1$):

$$\left(\frac{dT}{du_x}\right)^* \left[\left(\frac{dT}{du_x}\right)^* + \frac{7M_1^2}{36}\right] = 0 , \qquad (A7)$$

and which has the two roots

$$\left(\frac{dT}{du_x}\right)^* = 0 , -\frac{7M_1^2}{36} , \qquad (A8)$$

of which only the latter has physical significance.

In order to begin numerical integration it was first assumed, quite arbitrarily, that we were at the point where $\Delta u_x = 1/100 << 1/4$; the consistent value of the temperature perturbation is, from the linearized analysis, $\Delta T \cong (dT/du_x)^* \cdot \Delta u_x = -7M_1^2/3600$. The initial values of u_x and T used to start numerical integration at this point follow immediately from Eq. (A 3); furthermore, it was assumed that $x = 0$ here, in order to match the relaxation zone solution which (as discussed in Sec. 5) proceeds by forward integration from $x = 0$ toward $x \rightarrow +\infty$. Integration of Eqs. (A1) and (A 2) was carried out in physical space by conventional numerical techniques from $x = 0$ toward $x = -\infty$ until the velocity and temperature came arbitrarily close to their upstream values $u_x = T = 1$. In these calculations the temperature-dependence of the Reynolds number was given by $R_e(T) = 1.65\, M_1\, T^{-3/4}$ as indicated, for un-ionized argon, by Eq. (60b).

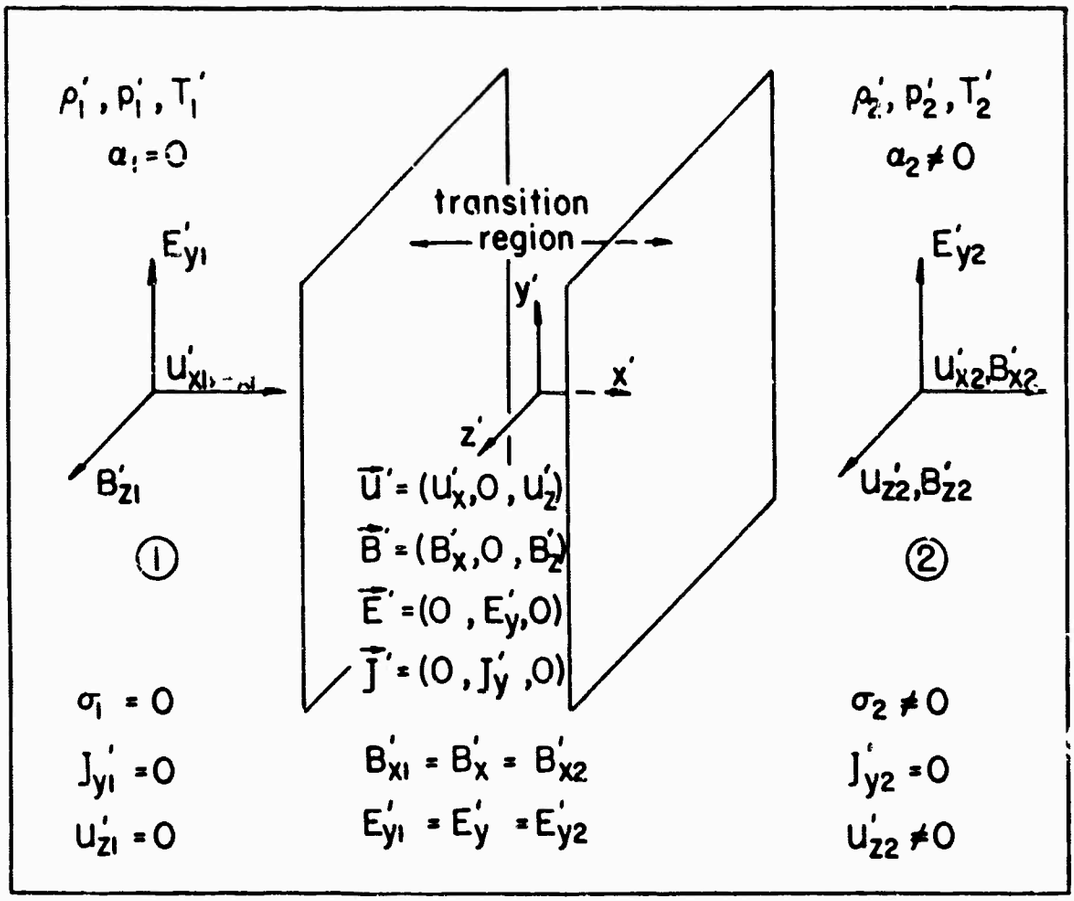

Fig. 1. **Sketch of gas-ionizing shock structure geometry in an oblique magnetic field. The cartesian (x', y', z') coordinate system is shock-fixed. The "primes" denote physical (dimensional) quantities.**

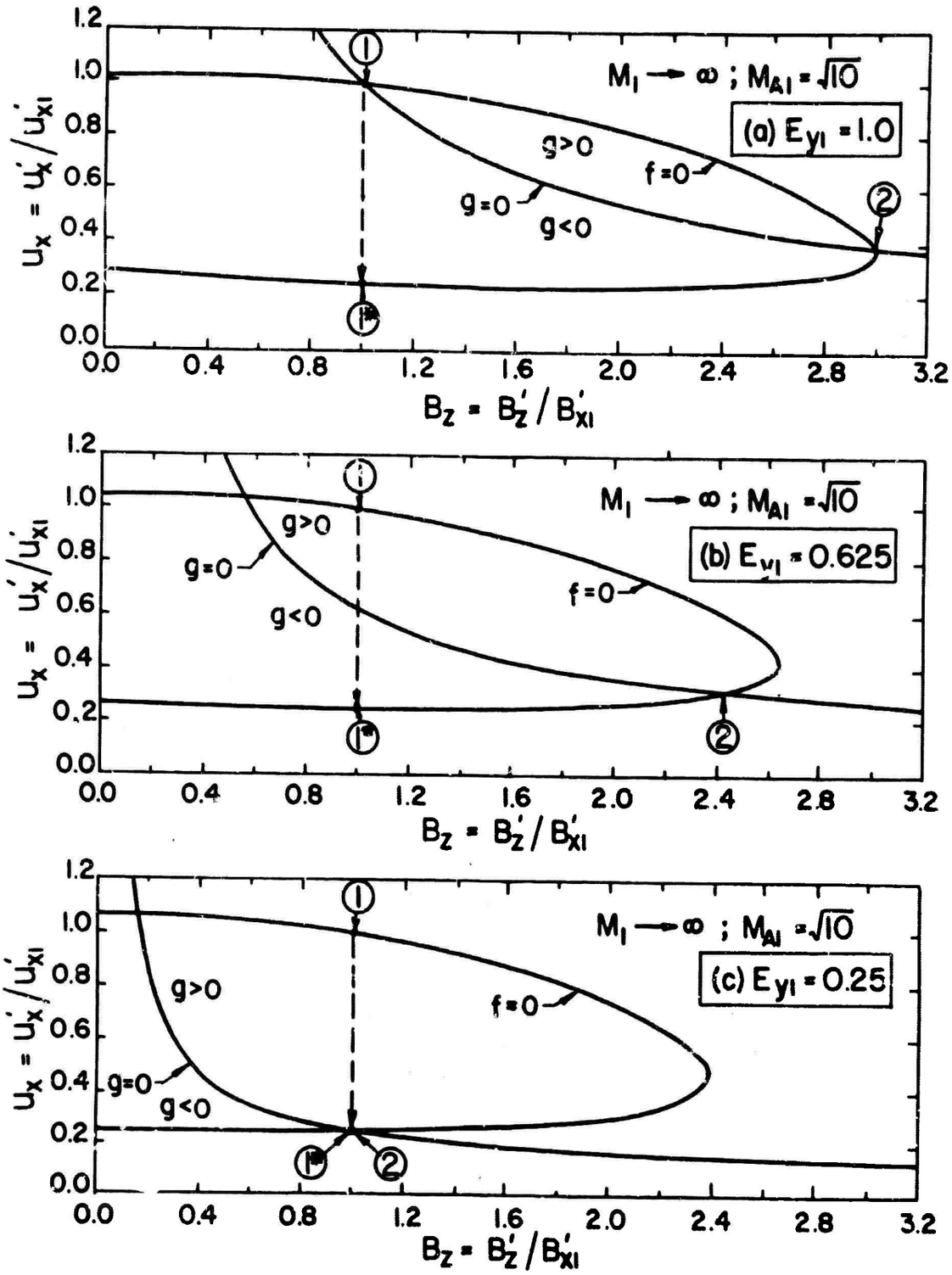

Fig. 2. Integral curves in (u_x, B_z) phase space for fast ($M_1 \to \infty$, $M_{A_1} = \sqrt{10}$) gas-ionising shocks of the 45° upstream magnetic field family ($B_{x_1} = B_{z_1} = 1$). Of the three electric fields shown, (a) $E_{y_1} = 1.0$, (b) $E_{y_1} = 0.625$, (c) $E_{y_1} = 0.25$, only "(c)" admits a solution in the ZND approximation. This is actually a degenerate case of a hydrodynamic shock.

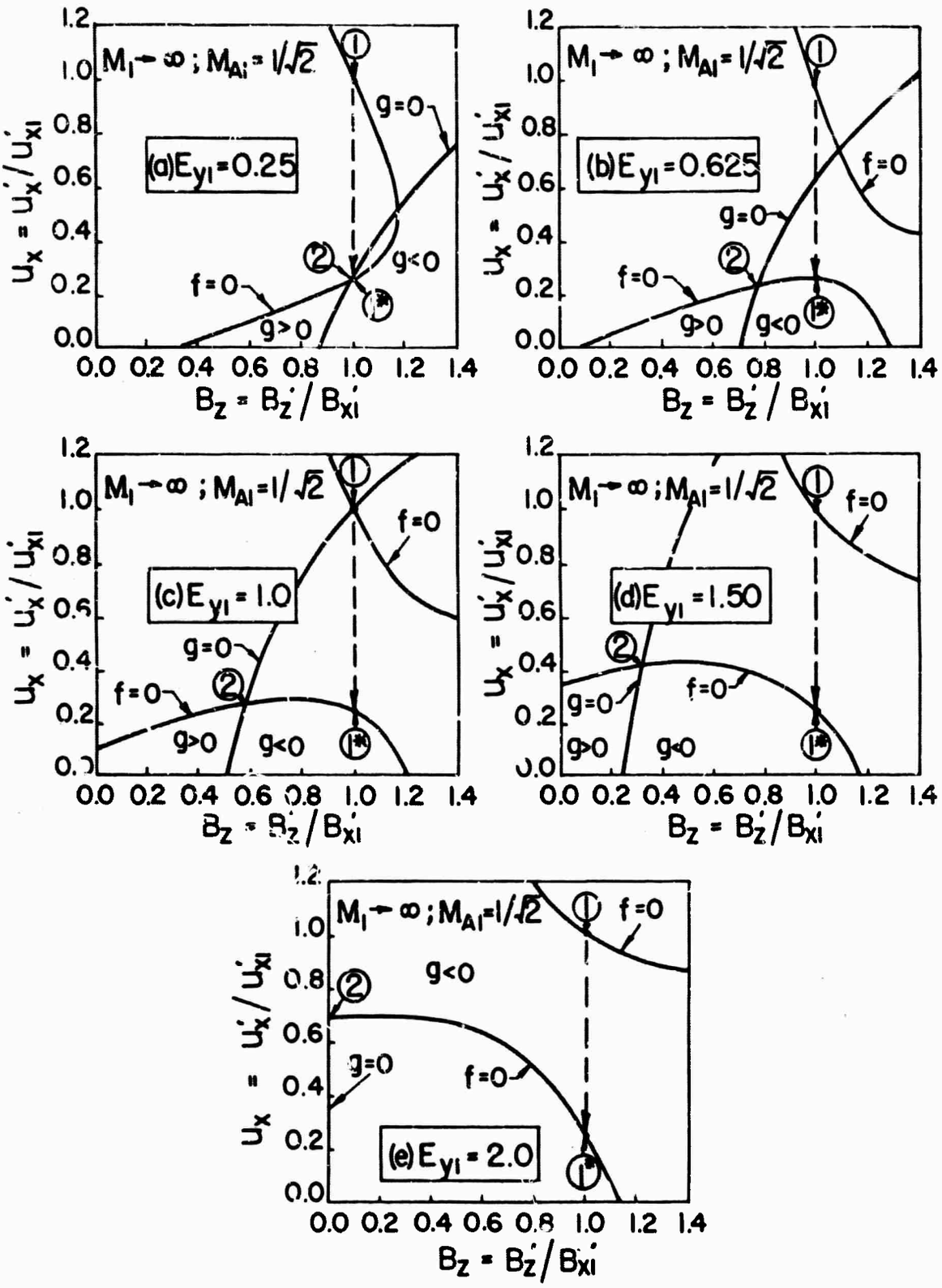

Fig. 3. Integral curves in (u_x, B_z) phase space for slow ($M_1 \to \infty$, $M_{A1} = 1/\sqrt{2}$) gas-ionizing shocks of the 45° upstream magnetic field family ($B_{x_1} = B_{z_1} = 1$). All five electric fields shown, (a) $E_{y_1} = 0.25$, (b) $E_{y_1} = 0.625$, (c) $E_{y_1} = 1.0$, (d) $E_{y_1} = 1.50$, (e) $E_{y_1} = 2.0$, will admit solutions in the ZND approximation. Case "(e)" is the new "gas-ionizing switch-off shock" discussed in the text.

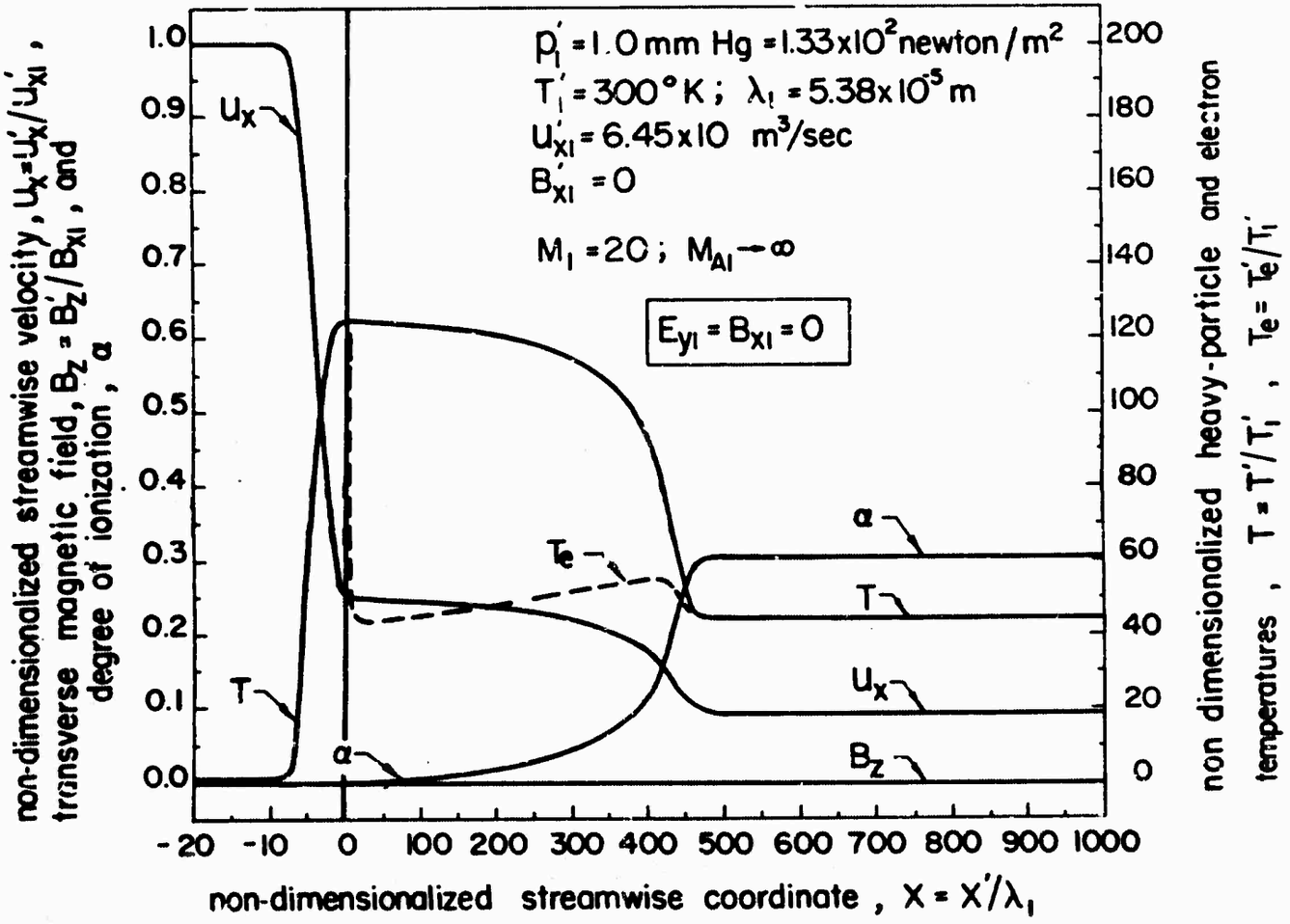

Fig. 4. Nonequilibrium structure of a pure hydrodynamic shock front ($B_{x_1} = B_{z_1} = E_{y_1} = 0$) propagating into un-ionized argon at pressure of $p_1' = 1.0$ mm Hg, temperature of $T_1' = 300°K$, at $M_1 = 20$ computed with the ZND approximation. The scale has been stretched by a factor of ten for $x<0$ compared to $x>0$ to show the imbedded Navier-Stokes viscous shock more clearly.

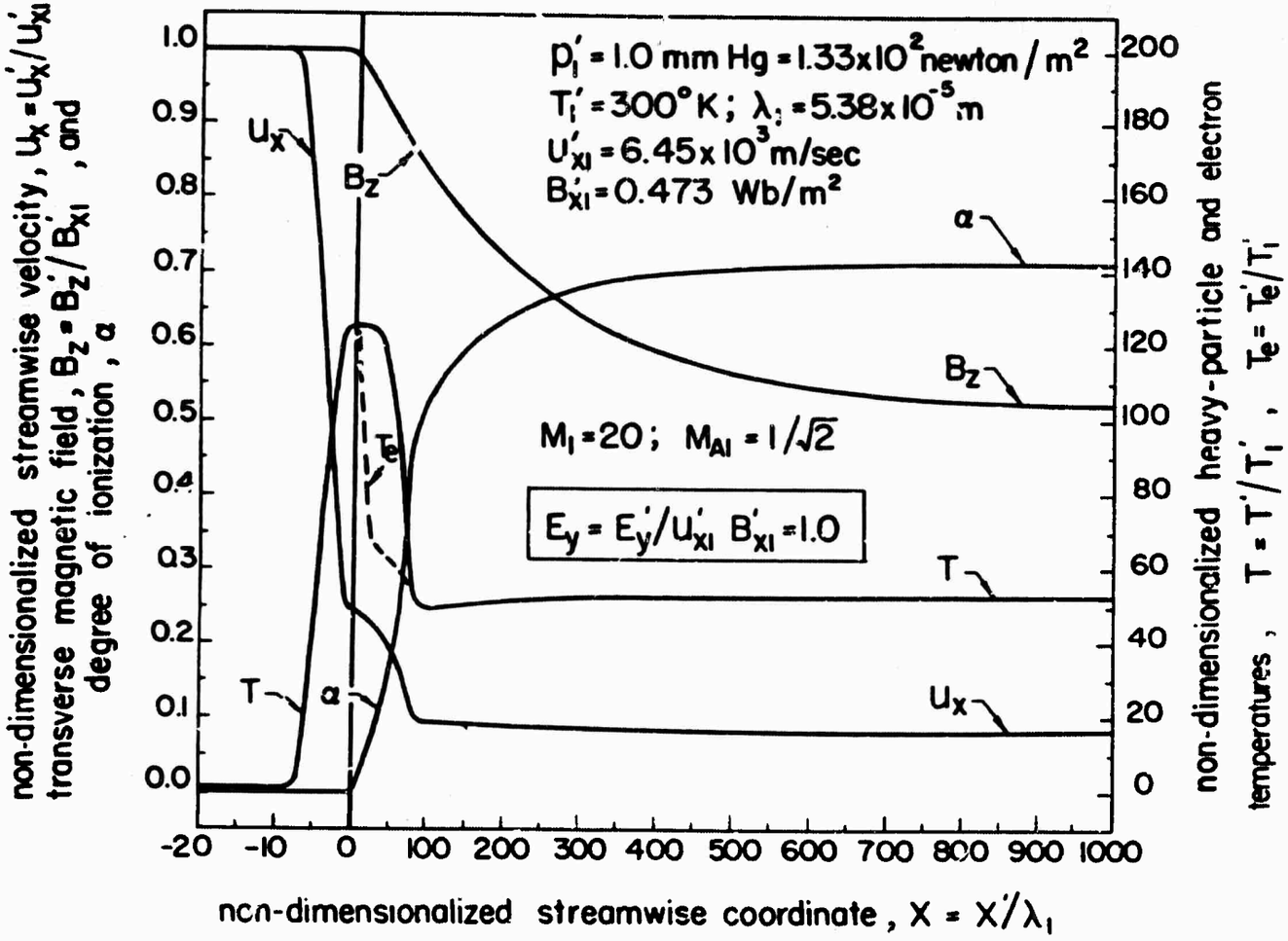

Fig. 5. Nonequilibrium structure of a slow ($M_1 = 20$, $M_{A_1} = 1/\sqrt{2}$) gas-ionizing shock front, of the 45° upstream magnetic field family ($B_{x_1} = B_{z1} = 1$), propagating into un-ionized Argon at a pressure $p_1' = 1.0$ mm Hg and temperature $T_1' = 300°K$ computed with the ZND approximation for $E_{y_1} = 1.0$. This case corresponds to the pure hydromagnetic boundary condition on the electric field. The scale has been stretched by a factor of ten for $x<0$ compared to $x>0$ to show the imbedded Navier-Stokes viscous shock more clearly.

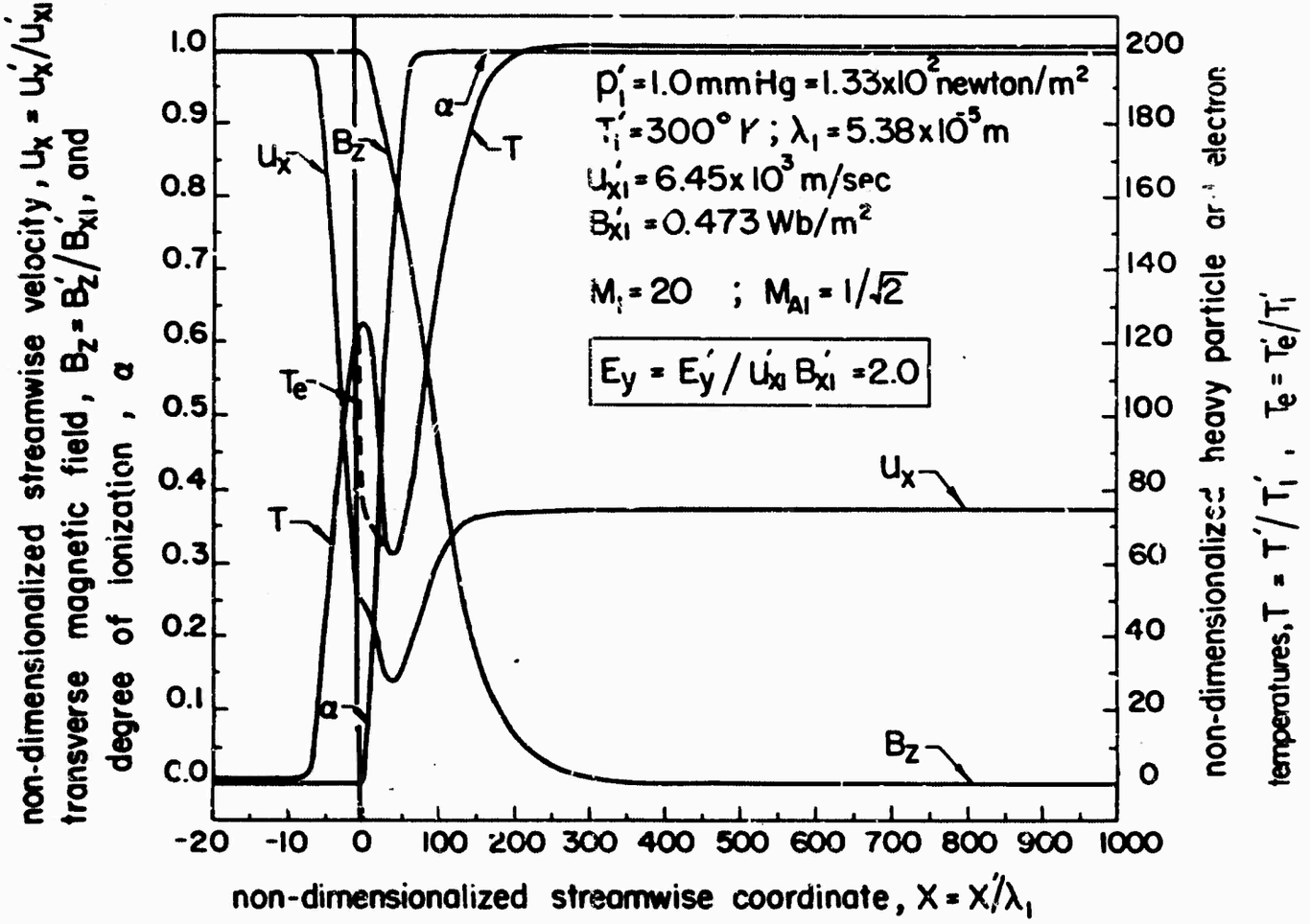

Fig. 6. Nonequilibrium structure of a slow ($M_1 = 20$, $M_{A1} = 1/\sqrt{2}$) gas-ionizing shock front, of the 45° upstream magnetic field family ($B_{x_1} = B_{z_1} = 1$), propagating into un-ionized argon at a pressure $p_1' = 1.0$ mm Hg and temperature $T_1' = 300°$K computed with the ZND approximation for $E_{y_1} = 2.0$. This is a "gas-ionizing switch-off shock". The scale has been stretched by a factor of ten for $x<0$ compared to $x>0$ to show the imbedded Navier-Stokes viscous shock more clearly.

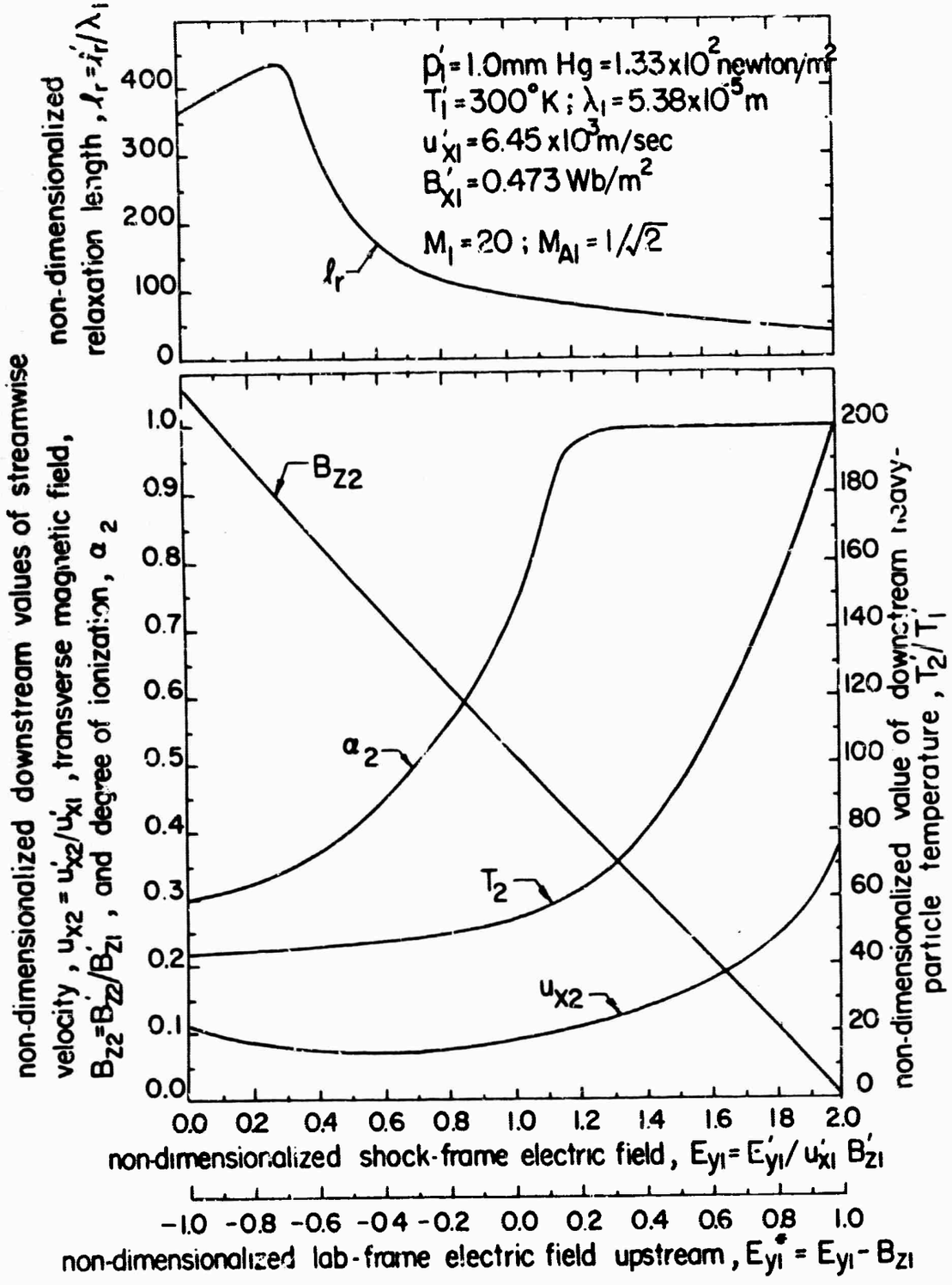

Fig. 7. Variation of nondimensionalized downstream streamwise velocity u_{x_2}, transverse magnetic field, B_{z_2}, degree of ionization α_2 and nondimensionalized relaxation length l_r, for various shock-frame (and corresponding lab-frame) electric fields for a slow shock with $M_1 = 20$, $M_{A_1} = 1/\sqrt{2}$, $p_1 = 1.0$ mm Hg and temperature $T_1 = 300°K$. A unique value of the electric field is not defined by the structure.

Advanced Research Projects Agency
Attn: Dr. David C. Mann
The Pentagon
Washington, D.C. 20301

Advanced Research Projects Agency
Attn: Lt.Col. R.M. Dowe, Jr.
The Pentagon
Washington, D.C. 20301

Advanced Research Projects Agency
Attn: Mr. C.E. McLain
The Pentagon
Washington, D.C. 20301

Advanced Research Projects Agency
Attn: Mr F.A. Keother
The Pentagon
Washington, D.C. 20301

Advanced Research Projects Agency
Attn: Dr. P.L. Auer
The Pentagon
Washington, D.C. 20301

Advanced Research Projects Agency
Attn: Dr. R. Zirkind
The Pentagon
Washington, D.C. 20301

Advanced Research Projects Agency
Attn: Maj. H. Dickinson
The Pentagon
Washington, D. C. 20301

Aerojet-General Corporation
Attn: Technical Library
P.O. Box 296
Azusa, California 91703

Philco Corporation
Aeronutronic Division
Attn: Dr. H. Shenfield
Ford Road
Newport Beach, Calif. 92600

Aerospace Corporation
Attn: Mgr., Penetration Aids
2400 E. El Segundo Blvd.
El Segundo, Calif.

Aerospace Corporation
Attn. Mr. William Barry
Norton Air Force Base
San Bernardino, Calif.

Air Force Cambridge Research Laboratories
Attn: Scientific Library
CRRELR, Stop 29
L.G. Hanscom Field
Bedford, Mass.

Air Force Cambridge Research Laboratories
Attn: Dr. Norman W. Rosenberg
L.G. Hanscom Field
Bedford, Mass.

Air Force Cambridge Research Laboratories
Attn: Dr. K. Champion
L.G. Hanscom Field
Bedford, Mass.

Air Force Cambridge Research Laboratories
Attn: Dr. A.T. Stair (CROR)
L.G. Hanscom Field
Bedford, Mass.

Air Force Office of Scientific Research
Attn: Dr. M.C. Harrington
1400 Wilson Blvd.
Arlington, Virginia 22209

Air Force Office of Scientific Research
Attn: Dr. D.L. Wennersten
1400 Wilson Blvd.
Arlington, Virginia 22209

Army Missile Command
Attn: AMCPM-ZER-R
Redstone Arsenal
Huntsville, Alabama 35808

Army Missile Command
Attn: AMSMI-RB
Redstone Arsenal
Huntsville, Alabama 35808

Army Missile Command
Attn: AMSMI-RNM
Redstone Arsenal
Huntsville, Alabama 35808

Army Research Office
Attn: Dr. Hermann Robl
Box C.M. Duke Station
Durham, N.C. 27706

Army Technical Intelligence Agency
Attn: ORDLI
Arlington Hall Station
Arlington, Virginia 22314

Air Force Weapons Laboratory
Attn: Capt. David Sparks
Kirtland Air Force Base
Albuquerque, N.M.

Air Force Weapons Laboratory
Attn: Capt. William Whittaker
Kirtland Air Force Base
Albuquerque, N.M.

Applied Physics Laboratory
Johns Hopkins University
Attn: Dr. Felix Falls
8621 Georgia Avenue
Silver Spring, Md. 20910

Arecibo Ionospheric Observatory
Attn: Dr. W.E. Gordon, Dir.
Box 995
Arecibo, Puerto Rico

Australian Embassy
Attn: D. Barnsley, Defense R. and E. Representative
2001 Connecticut Ave., NW
Washington, D.C. 20008

Avco-Everett Research Lab.
Attn: Technical Library
2385 Revere Beach Pkwy.
Everett, Mass. 02149

Avco-Everett Research Lab.
Attn: Mr. P. Rose
2385 Revere Beach Pkwy.
Everett, Mass. 02149

Avco-Research and Advanced Development Div.
Attn: Mr. Harold Debolt
201 Lowell Street
Wilmington, Mass. 01887

Avco-Research and Advanced Development Div.
Attn: Dr. A. Pallone
201 Lowell Street
Wilmington, Mass. 01887

Ballistics Research Laboratory
Attn: Dr. C.H. Murphy
Aberdeen Proving Ground, Md. 21005

Battelle Memorial Institute
Attn: Battelle-DEFENDER
505 King Avenue
Columbus, Ohio 43201

Bell Telephone Laboratories
Attn: Dr. C. W. Hoover
Whippany, N. J. 07981

Bendix Systems Division
Flight Sciences Department
Ann Arbor, Michigan

British Joint Mission
British Embassy
Attn: Mr. A. N. Mosses
Defense Research Staff
3100 Massachusetts Ave., NW
Washington, D. C. 20008

Brown University
Attn: Dr. John Ross
Department of Chemistry
Providence, Rhode Island 02912

Bureau of Naval Weapons
Special Projects Office
Attn: Comdr. Julian, SP-25
Munitions Bldg.
Washington, D. C. 20360

Canadian Armament Research
and Development Establish.
Attn: U. S. Army Liaison Ofcr.
P. O. Box 1427
Quebec, P. Q., Canada

Air Force Cambridge Research
Laboratories
CRUB
Attn: Dr, K. Champion
Bedford, Mass.

Central Intelligence Agency
Attn: OCR Standard Distribution
2430 E St., NW
Washington, D. C. 20505

Chief of Naval Operations
Attn: OP-07TIO
Washington, D. C.

Dr. A. Hertzberg
Director, Aero. Lab.
University of Washington
Seattle, Wash. 98105

Cornell University
Nuclear Studies Laboratory
Attn: Dr. Edwin E. Salpeter
Ithaca, N. Y. 14850

Defense Atomic Support Agency
Attn: Dr. T. Taylor
Deputy Director, Scientific
The Pentagon, 1 B 697
Washington, D. C.

Defense Atomic Support Agency
Attn: Dr. C. Blank
The Pentagon, 1 B 697
Washington, D. C.

Defense Documentation Center
Cameron Station
Alexandria, Virginia 22314

50 copies

Defense Research Corporation
Attn: Dr. Bernard A. Lippmann
P. O. Box 3586
Santa Barbara, Calif.

U. S. Naval Postgraduate School
Attn: Tech. Reports Library
Monterey, Calif. 93940

General Applied Science Labs.
Attn: Library
Merrick and Stewart Avenues
Wesbury, L. I., N. Y. 11590

General Applied Science Labs.
Attn: Dr. Lewis Feldman
Merrick and Stewart Avenues
Westbury, L. I., N. Y. 11590

RCA-Victor Co., Ltd.
Research Laboratories
Attn: Dr. A. I. Carswell
1001 Lenoir Street
Montreal 30, Canada

General Dynamics Corporation
Convair Division
Attn: Mr. K. G. Blair
Chief Librarian
P. O. Box 166
San Diego, California 92112

General Dynamics Corporation
Convair Division
Attn: Dr. Roy H. Neynaber
P. O. Box 166
San Diego, Calif. 92112

Commanding Officer
U. S. Naval Weapons Lab.
Dahlgren, Virginia 22448

General Electric Co., MSVD
Document Library
Reentry Physics Library Unit
Attn: Mgr., MSVD Library 3446
3198 Chestnut Street
Philadelphia, Pa.

General Electric Research Lab.
Attn: Dr. George C. Baldwin
(Gen. Engrg. Lab.)
Schenectady, N. Y. 12301

General Electric Space Sciences
Laboratory
Attn: Dr. T. Reithoff
Valley Forge Space Tech. Ctr.
P. O. Box 8555
Valley Forge, Pa.

General Electric Tem...
Attn: ... R. Hendrick
Santa Barbara, California

General Motors
Defense Research Laboratory
Attn: Mr. C. M. S... r
Box T
Santa Barbara, California 93102

Geophysics Corp. of America
Burlington Road
Bedford, Mass.

Harvard University
Chemistry Department
Attn: Dr. D. R. Hershbach
Cambridge, Mass. 02138

Headquarters BSD (AFSC)
Air Force Unit Post Office
Attn: BSRVD
Los Angeles, Calif. 90045

Heliodyne Corporation
Attn: Dr. Saul Feldman
7810 Burnet Avenue
Van Nuys, Calif. 91405

Illinois Institute of Technology
Research Institute
Attn: Dr. Carsten Haaland
10 West 35th Street
Chicago, Ill. 60616

Dr. W. Culver
International Business Machines
326 E. Montgomery Avenue
Rockville, Maryland

Institute for Defense Analyses
Attn: Dr. A. Hochstim
400 Army-Navy Drive
Arlington, Virginia 22202
2 copies

Institute for Defense Analyses
Attn: Dr. D. Katcher
JASON Library
400 Army-Navy Drive
Arlington, Virginia 22202

Institute for Defense Analyses
Attn: Dr. J. Menkes
400 Army-Navy Drive
Arlington, Virginia 22202

Institute for Defense Analyses
Attn: Dr. H. Wolfhard
400 Army-Navy Drive
Arlington, Virginia 22202

Institute for Molecular Physics
Attn: Dr. Edward A. Mason
University of Maryland
College Par', Md.

Joint Inst. for Lab. Astrophysics
NBS, University of Colorado
Attn: Dr. Lewis Branscomb
1511 University Avenue
Boulder, Colorado

Jet Propulsion Laboratory
Attn: Library
4800 Oak Grove Drive
Pasadena, Calif. 91103

Kansas State University
Attn: Prof. Basil Curnutte
Physics Department
Manhattan, Kansas

Lincoln Laboratory, M.I.T.
Attn: Dr. M. Balser
P.O. Box 73
Lexington, Mass. 02173

Lockheed Missiles and Space Co.
Attn: Dr. R. Myerott
3251 Hanover Street
Palo Alto, Calif.

Lockheed Missiles and Space Co.
Attn: Dr. Leon Fisher
3251 Hanover Street
Palo Alto, California

Monsanto Research Corporation
Dayton Laboratory
Attn: Dr. J.W. Butler
1515 Nicholas Road
P.O. Box 8, Station B
Dayton, Ohio

Naval Ordnance Laboratory
Attn: Librarian
White Oak
Silver Spring, Md. 20910

Naval Research Laboratory
Attn: Dr. Alan Kolb, Code 7470
Washington, D.C. 20390

Naval Research Laboratory
Attn: Code 2027
Washington, D.C. 20390
(6)

National Aeronautics and Space Administration
Attn: Applied Materials and Physics Div., Code SL
Langley Research Center
Hampton, Virginia 23365

National Aeronautics and Space Administration
Attn: Mail Stop 213
Langley Research Center
Hampton, Virginia 23365

Radio Corporation of America
Missile and Surface Radar Div.
Moorestown, N.J. 08057

Director
Naval Research Laboratory
Washington, D.C. 20390
Attn: Dr. R.M. Page

National Bureau of Standards
Attn: Dr. Karl G. Kessler, Chief
Atomic Physics Division
Washington, D.C. 20234

National Bureau of Standards
Attn: Dr. M.E. Wallenstein
Chief, Physical Chem. Div.
Washington, D.C. 20234

National Bureau of Standards
Attn: Dr. Kurt E. Shuler
Washington, D.C. 20234

National Bureau of Standards
Attn: Dr. E.L. Brady
National Standard Reference Data Center
Washington, D.C. 20234

New York University
Attn: Dr. Benjamin Bederson
Physics Department
University Heights
New York, N.Y. 10453

New York University
Attn: Dr. Sidney Borowitz
Physics Department
University Heights
New York, N.Y. 10453

Oak Ridge National Laboratory
Attn: Dr. S. Datz
P.O. Box X
Oak Ridge, Tenn.

Office of Naval Research
Department of the Navy
Attn: Dr. S.G. Reed, Jr.
Science Director
Washington, D.C. 20360

Office of Naval Research
Department of the Navy
Attn: Dr. J.H. Shenk
Materials Science Div.
Washington, D.C. 20360

Office of Naval Research
Department of the Navy
Attn: Dr. W.E. Wright
Physical Sciences Div.
Washington, D.C. 20360

Office of Naval Research
Department of the Navy
Attn: Dr. F.T. Byrne
Physics Section
Washington, D.C. 20360

Polytechnic Institute of Brooklyn
Attn: Mr. Jerome Fox
Research Office
333 Jay Street
Brooklyn, N.Y. 11201

Queen's University of Belfast
Attn: Professor D.R. Bates
Department of Applied Math.
Belfast 7, Northern Ireland, UK

The Rand Corporation
Attn: Library
1700 Main Street
Santa Monica, Calif. 90401

The Rand Corporation
Attn: Dr. R. Hundley
1700 Main Street
Santa Monica, Calif. 90401

The Rand Corporation
Attn: Dr. F. R. Gilmore
1700 Main Street
Santa Monica, Calif. 90401

The Rand Corporation
Attn: Dr. R. E. LeLevier
1700 Main Street
Santa Monica, Calif. 90401

Rocketdyne Division
North American Aviation, Inc.
Attn: Dr. S. A. Golden
Physics Group
6633 Canoga Avenue
Canoga Park, Calif. 91304

Sperry Rand Research Center
Attn: Dr. Philip M. Stone
North Road (Route 117)
Sudbury, Mass.

Space Technology Laboratories
Attn: Dr. L. Hromas
1 Space Park
Redondo Beach, Calif. 90200

Stanford Research Institute
Attn: Dr. C. J. Cook, Director
Chemical Physics Division
333 Ravenswood Avenue
Menlo Park, Calif. 94025

Chief of Naval Research
Department of the Navy
Code 427
Washington, D. C. 20360

Commanding Officer
U. S. Naval Electronics Lab.
San Diego, Calif. 92152

Commanding Officer and Dir.
U. S. Naval Training Device
Center
Attn: Technical Library
Orlando, Florida 32813

Stanford Research Institute
Attn: Dr. C. Flammer, Mgr.
Mathematical Division
333 Ravenswood Avenue
Menlo Park, Calif. 94025

United Aircraft Corporation
Research Laboratories
Attn: Dr. R. G. Meyerand
East Hartford, Conn. 06118

University of Alabama
Attn: Dr. Erich Rodgers
Physics Department
P. O. Box 1921
University, Alabama 48106

University of California
Attn: Prof. Kenneth Watson
Physics Department
Berkeley, Calif. 94704

University of California
Lawrence Radiation Laboratory
Attn: Dr. Marvin Mittleman
Box 808
Livermore, Calif. 94551

University of California
Attn: Dr. Herbert P. Broida
Department of Physics
Santa Barbara, Calif.

Dr. Keith A. Brueckner
University of California
San Diego
P. O. Box 109
La Jolla, Calif. 92038

University of Chicago
Attn: Dr. John Light
Chemistry Department
Chicago, Illinois

Commanding Officer
Naval Ordnance Test Station
China Lake, Calif. 93357

Commanding Officer
U. S. Naval Avionics Facility
Indianapolis, Indiana

Commanding Officer
Office of Naval Research
Box 39
FPO, New York, N.Y. 09510

University of Chicago
Attn: Prof. C. C. J. Roothaan
Department of Physics
Chicago, Ill.

University of Florida
Attn: Dr. Alex Green
Physics Department
Gainesville, Florida 32603

University of Michigan
Attn: Dr. R. Bernstein
Chemistry Department
Ann Arbor, Michigan 48106

University of Michigan
Attn: Dr. Otto LaPorte
Physics Department
Ann Arbor, Michigan 48106

University of Minnesota
Attn: Prof. H. J. Oskam
Department of Electrical
Engineering
Institute of Technology
Minneapolis, Minn. 55414

University of Pittsburgh
Attn: Professor Wade Fite
Pittsburgh, Pa. 15214

University of Southern Calif.
Attn: Prof. G. L. Weissler
Department of Physics
University Park
Los Angeles, Calif. 90007

Westinghouse Electric Corp.
Attn: Dr. A. Phelps
Research Laboratories
Pittsburgh, Pa.

Commanding Officer
Office of Naval Research
Branch Office
207 West 24th Street
New York, N. Y. 10011

Commanding Officer
Naval Ordnance Test Station
Corona, Calif. 91720

Dr. Luigi Crocco
Princeton University
Forrestal Research Center
Princeton, New Jersey 08540

Dr. Milton Van Dyke
Dept. of Aeronautics and
Astronautics
Stanford University
Stanford, California 94305

AVCO-Everett Research Lab.
Attn: Research Library
(Route to Dr. F.R. Riddell)
201 Lowell Street
Wilmington, Massachusetts
01887

Dr. Adrian Pallone
AVCO Research & Advanced Dev.
Division
201 Lowell Street
Wilmington, Massachusetts
01887

Convair Scientific Research Lab
Attn: Library
(Route to Chief, Appl.Research)
P. O. Box 950
San Diego, California 92112

Dr. Henry Lew
General Electric Company
Space Sciences Laboratory
Valley Forge Space Tech. Center
King of Prussia, Pennsylvania
19406

DATAC, Research Laboratory
The Martin Company
P. O. Box 179
Denver, Colorado 80201

RIAS, Inc.
Attn: Library
1450 S. Rolling Road
Baltimore, Maryland 21227

Dr. Philip M. Mostov
Electrical Engineering Dept.
University of Pittsburgh
Pittsburgh, Pennsylvania
15213

Dr. R. Goulard
Purdue University
School of Aero. & Engineering Sci.
Lafayette, Indiana 47907

Stanford University
Dept. of Aeronautical Engineering
Attn: Library
Stanford, California 94305

AVCO-Everett Research Lab.
Attn: Technical Library
(Route to Dr. H.E. Petschek)
2385 Revere Beach Parkway
Everett, Massachusetts 02149

Aerojet Engineering Corp.
Attn: Chief, Technical Library
635 N. Irwindale Avenue
Box 296
Azusa, California 91703

General Applied Science Labs.Inc.
Attn: Library
Merrick & Stewart Avenues
Westbury, New York 11950

Republic Aviation Corp.
Attn: Reentry Simulation Lab.
Route 110
Farmingdale, New York 11735

Marquardt Aircraft Corporation
Attn: Library
Van Nuys, California 91404

Dr. N. Ness
Dept. of Aeronautical Engineering
University of West Virginia
Morgantown, West Virginia 26506

Engineering Societies Library
345 East 47th Street
New York, New York 10017
Attn: Acquisitions Dept.

Rensselaer Polytechnic Instit.
Dept. of Aeronautical Engine
Attn: Library
Troy, New York 12180

Dr. J. Lukasiewicz
Chief, von Karman Gas Dynamic
Facility
ARO, Inc.
Arnold Air Force Station
Tennessee 37389

Mr. Philip Levine, Chief
Aerodynamics Staff
AVCO Research & Advanced Dev.
201 Lowell Street
Wilmington, Massachusetts
01887

Boeing Scientific Research La
Attn: Research Library
P. O. Box 3981
Seattle, Washington 98124

MSVD Library
General Electric Company
Attn: L. Chasen, Mgr.-Library
Valley Forge Space Tech. Cent
King of Prussia, Pennsylvania
1940

Dr. S. Feldman, President
Heliodyne Corporation
7810 Burnet Avenue
Van Nuys, Calif. 91405

North American Aviation, Inc.
Attn: Mr. H.H. Crotsley, Chie
Aero. Sciences
Los Angeles International Air
Los Angeles, California 9004

Ramo-Wooldridge
Div. of Thompson-Ramo-Wooldr
8433 Fallbrook Avenue
Canoga Park, California 9130

FINAL MAILING LIST

NASA
Attn: Dr. H. H. Kurzweg
400 Maryland Ave., S.W.
Washington, D. C. 20546

Southwest Research Institute
Attn: Applied Mechanics Reviews
8500 Culebra Road
San Antonio, Texas 78228

California Institute of Tech.
Attn: JPL Library
4800 Oak Grove Drive
Pasadena, California 91102

Cornell Aeronautical Lab., Inc.
Attn: Library
4455 Genesee Street
Buffalo, New York 14221

Harvard University
Department of Applied Physics
Attn: Library
(Route to Prof. H. W. Emmons)
Cambridge, Massachusetts 02138

Illinois Institute of Technology
Armour Research Foundation
Attn: Library
Chicago, Illinois 60616

University of Maryland
Attn: Engineering Library
College Park, Maryland 20742

Dr. R. F. Probstein
Massachusetts Inst. of Technology
Dept. of Mechanical Engineering
Cambridge, Massachusetts
02139

University of Minnesota
Institute of Technology
Attn: Engineering Library
Minneapolis, Minnesota 55414

Pennsylvania State University
Dept. of Aeronautical Eng.
Attn: Library
University Park, Pa.
16802

Chief, Bureau of Naval Weapons
Department of the Navy
Attn: Research Division
Washington, D. C. 20360

NASA
Langley Research Center
Attn: Dr. J.V. Becker
Chief, Aero-Physics Div.
Langley Field, Hampton, Virginia
23365

University of California
Engineering Department
Library
Los Angeles, California 90024

California Inst. of Technology
Attn: Prof. Lester Lees
Dept. of Aeronautics
Pasadena, California 91102

Cornell University
Graduate School of Aero. Eng.
Attn: Library
(Route to Prof. W. R. Sears)
Ithaca, New York 14850

The Johns Hopkins University
Applied Physics Laboratory
Attn: Library
8621 Georgia Avenue
Silver Spring, Maryland 20910

University of Illinois
Aeronautical Institute
Attn: School of Engineering
Urbana, Illinois 61803

Massachusetts Inst. of Technology
Attn: Aeronautics Library
Cambridge, Massachusetts
02139

University of Michigan
Dept. of Aero. Engineering
Attn: Library
East Engineering Building
Ann Arbor, Michigan 48106

Rosemount Aeronautical Labs.
University of Minnesota
Attn: Library
Minneapolis, Minnesota 55414

Princeton University
Dept. of Aeronautical Eng.
Attn: Library
Princeton, New Jersey 08540

Institute for Defense Analyses
Attn: Director of Defense Research
400 Army-Navy Drive
Arlington, Virginia 22202

International Aerospace Abstracts
1290 Avenue of the Americas
New York, New York 10019

Dr. Nicholas Rott
University of California
Los Angeles, California 90024

California Inst. of Technology
Guggenheim Aeronautical Lab.
Attn: Aeronautics Library
(Route to Prof. Liepmann)
Pasadena, California 91102

Harvard University
Dept. of Engineering Sciences
Attn: Library
Cambridge, Massachusetts
02138

The Johns Hopkins University
Department of Mechanics
Attn: Library
(Route to Profs. Clauser &
Corrsin)
Baltimore, Maryland 21218
University of Maryland
Institute of Fluid Dynamics
and Applied Mathematics
College Park, Maryland 20742

Massachusetts Inst. of Technolog
Fluid Dynamics Research Group
Attn: Dr. Leon Trilling
Cambridge, Massachusetts
02139

Ballistic Missile Radiation
Analysis Center
University of Michigan
Ann Arbor, Michigan 48106

Ohio State University
Dept. of Aeronautical Eng.
Attn: Library
Columbus, Ohio 43210

The James Forrestal Research Ctr
Princeton University
Attn: Library
(Route to Prof. S. Bogdonoff)
Princeton, New Jersey 08540

Unclassified
Security Classification

DOCUMENT CONTROL DATA - R&D
(Security classification of title, body of abstract and indexing annotation must be entered when the overall report is classified)

1. ORIGINATING ACTIVITY (Corporate author)
Polytechnic Institute of Brooklyn
Dept. of Aerospace Engrg. and Applied Mechanics

2a. REPORT SECURITY CLASSIFICATION
Unclassified

2b. GROUP

3. REPORT TITLE
NONEQUILIBRIUM STRUCTURE OF HYDROMAGNETIC GAS-IONIZING SHOCK FRONTS IN ARGON

4. DESCRIPTIVE NOTES (Type of report and inclusive dates)
Research report

5. AUTHOR(S) (Last name, first name, initial)
Hoffert, Martin I.

6. REPORT DATE	7a. TOTAL NO. OF PAGES	7b. NO. OF REFS
February 1967	54	41

8a. CONTRACT OR GRANT NO.	9a. ORIGINATOR'S REPORT NUMBER(S)
Nonr 839(38)	PIBAL Report No. 1008
b. PROJECT NO.	
c. ARPA Order No. 529	9b. OTHER REPORT NO(S) (Any other numbers that may be assigned this report)
d.	

10. AVAILABILITY/LIMITATION NOTICES
Distribution of this document is unlimited. Qualified requesters may obtain copies from DDC.

11. SUPPLEMENTARY NOTES	12. SPONSORING MILITARY ACTIVITY
	Office of Naval Research - Code 438 Department of the Navy Washington, D.C. 20360

13. ABSTRACT

This study deals analytically with the structure of gas-ionizing hydromagnetic shock waves. Since these waves, by definition, must have non-electrically-conducting upstream states, their existence at very high shock temperatures must be ruled out on the physical grounds that forward-radiated precursor ionization makes the unshocked gas conducting. A "low temperature" collisionally-ionizing shock with oblique magnetic field is studied here to determine whether certain concepts which exist in the current literature are relevant. Nondimensionalized equations governing the nonequilibrium structure of such a front propagating into un-ionized argon are formulated using ionization rates and an electron energy equation developed in an earlier paper. Comparison of the magnitudes of viscous and magnetic Reynolds numbers within this front indicates that, if a structure exists, it must consist of a narrow "imbedded" viscous shock standing upstream of a much wider hydromagnetic interaction and ionization relaxation zone. Hence, a modified form of the Zeldovich-von Neumann-Döring (ZND) approximation is applicable to the structure problem. It is shown that in this approximation non-trivial steady-state structures cannot be constructed for "fast" gas-ionizing shocks. On the other hand, solutions are possible for "slow" waves, and these are obtained numerically for a family of hydromagnetically oblique shocks at Mach number $M_1=20$ and Alfvén number $M_{A_1}=1/\sqrt{2}$ with parametrically varied values of the upstream electric field. In contrast to previous expectations, the upstream electric field is not uniquely defined by the structure.

DD FORM 1 JAN 64 1473

Unclassified
Security Classification

14. KEY WORDS	LINK A		LINK B		LINK C	
	ROLE	WT	ROLE	WT	ROLE	WT
Magnetohydrodynamic shock waves						
Nonequilibrium ionization						
Argon						
Electron temperature						
Precursor ionization						

INSTRUCTIONS

1. ORIGINATING ACTIVITY: Enter the name and address of the contractor, subcontractor, grantee, Department of Defense activity or other organization *(corporate author)* issuing the report.

2a. REPORT SECURITY CLASSIFICATION: Enter the overall security classification of the report. Indicate whether "Restricted Data" is included. Marking is to be in accordance with appropriate security regulations.

2b. GROUP: Automatic downgrading is specified in DoD Directive 5200.10 and Armed Forces Industrial Manual. Enter the group number. Also, when applicable, show that optional markings have been used for Group 3 and Group 4 as authorized.

3. REPORT TITLE: Enter the complete report title in all capital letters. Titles in all cases should be unclassified. If a meaningful title cannot be selected without classification, show title classification in all capitals in parenthesis immediately following the title.

4. DESCRIPTIVE NOTES: If appropriate, enter the type of report, e.g., interim, progress, summary, annual, or final. Give the inclusive dates when a specific reporting period is covered.

5. AUTHOR(S): Enter the name(s) of author(s) as shown on or in the report. Enter last name, first name, middle initial. If military, show rank and branch of service. The name of the principal author is an absolute minimum requirement.

6. REPORT DATE: Enter the date of the report as day, month, year; or month, year. If more than one date appears on the report, use date of publication.

7a. TOTAL NUMBER OF PAGES: The total page count should follow normal pagination procedures, i.e., enter the number of pages containing information.

7b. NUMBER OF REFERENCES: Enter the total number of references cited in the report.

8a. CONTRACT OR GRANT NUMBER: If appropriate, enter the applicable number of the contract or grant under which the report was written.

8b, 8c, & 8d. PROJECT NUMBER: Enter the appropriate military department identification, such as project number, subproject number, system numbers, task number, etc.

9a. ORIGINATOR'S REPORT NUMBER(S): Enter the official report number by which the document will be identified and controlled by the originating activity. This number must be unique to this report.

9b. OTHER REPORT NUMBER(S): If the report has been assigned any other report numbers *(either by the originator or by the sponsor)*, also enter this number(s).

10. AVAILABILITY/LIMITATION NOTICES: Enter any limitations on further dissemination of the report, other than those imposed by security classification, using standard statements such as:

(1) "Qualified requesters may obtain copies of this report from DDC."

(2) "Foreign announcement and dissemination of this report by DDC is not authorized."

(3) "U. S. Government agencies may obtain copies of this report directly from DDC. Other qualified DDC users shall request through

_____."

(4) "U. S. military agencies may obtain copies of this report directly from DDC. Other qualified users shall request through

_____."

(5) "All distribution of this report is controlled. Qualified DDC users shall request through

_____."

If the report has been furnished to the Office of Technical Services, Department of Commerce, for sale to the public, indicate this fact and enter the price, if known.

11. SUPPLEMENTARY NOTES: Use for additional explanatory notes.

12. SPONSORING MILITARY ACTIVITY: Enter the name of the departmental project office or laboratory sponsoring *(paying for)* the research and development. Include address.

13. ABSTRACT: Enter an abstract giving a brief and factual summary of the document indicative of the report, even though it may also appear elsewhere in the body of the technical report. If additional space is required, a continuation sheet shall be attached.

It is highly desirable that the abstract of classified reports be unclassified. Each paragraph of the abstract shall end with an indication of the military security classification of the information in the paragraph, represented as *(TS), (S), (C), or (U)*.

There is no limitation on the length of the abstract. However, the suggested length is from 150 to 225 words.

14. KEY WORDS: Key words are technically meaningful terms or short phrases that characterize a report and may be used as index entries for cataloging the report. Key words must be selected so that no security classification is required. Identifiers, such as equipment model designation, trade name, military project code name, geographic location, may be used as key words but will be followed by an indication of technical context. The assignment of links, rules, and weights is optional.

GPO 886-551